Analysis and prediction of MODIS LAI time series with Dynamic Harmonic Regression model

JIANG Bo[1,2], LIANG Shun-lin[3], WANG Jin-di[1,2], XIAO Zhi-qiang[1,2]

1. *State Key Laboratory of Remote Sensing Science, Jointly Sponsored by Beijing Normal University and Institute of Remote Sensing Applications, Chinese Academy of Sciences, Beijing* 100101, *China*;
2. *Research Center for Remote Sensing and GIS, School of Geography, Beijing Key Laboratory for Remote Sensing of Environment and Digital Cities, Beijing Normal University, Beijing* 100875, *China*;
3. *Department of Geography, University of Maryland, College Park, MD* 20742, *USA*

Abstract: Leaf Area Index (LAI) is one of the most important parameters in describing the dynamics of vegetation on land surfaces. LAI products have been produced from data of many remote sensing satellite sensors, such as the Moderate Resolution Imaging Spectroradiometer (MODIS). In this paper, we used the Dynamic Harmonic Regression (DHR) model to analyze the LAI time series products. The model can decompose the trend, seasonal and residuals components from the original time series, and predict the short-time LAI values. We use the DHR model to extract the time change information from the MODIS LAI time series products. The results show this method to be very effective in predicting the short-term LAI on the pixel basis.

Key words: leaf area index (LAI), time series, MODIS, DHR

CLC number: TP702 **Document code:** A

Citation format: Jing B, Liang S L, Wang J D, Xiao Z Q. 2010. LAI time series analysis and prediction with Dynamic Harmonic Regression model. *Journal of Remote Sensing*, **14**(1): 013—032

1 INTRODUCTION

Leaf Area Index (LAI) is defined as the total weight of plant leaves per unit area on land surface and is a useful index for the studies of plant photosynthesis and energy exchange. LAI is asscioated with terrestrial ecology, leaf biochemistry, evapotranspiration, the interception of light on the leaf canopy, and the net primary productivity. It is, one of the most important parameters in the study of ecosystem of the land surface (Zhao, 2003). There have been several LAI products that derived from satellite sensors nowadays, such as MODIS, SPOT, MERIS. Because of the revisiting characteristic of the satellite, a large amount of LAI time series data has been accumulated. By analyzing these time series remote sensing products, such as LAI, we can extract dynamic information about the landscape, especially the reasonable and interannual trends of vegetation canopies, which are significant in studies of both the dynamics of land surface and climate change. Consequently, the time series analysis of remote sensing products is extremely important.

MODIS (Moderate Resolution Imaging Spectral Radiometer) has 36 bands ranging from the visible to the thermal infrared spectrum and observes the Earth every eight days. The MODIS LAI product (MOD15A2) has a spatial resolution of 1km. Because of cloud, aerosol contaminations and other factors, the MODIS LAI product has missing values. Accordingly, a method that can extract the useful information from the LAI time series, eliminate the noises, model the temporal variations and predict the future values is necessary.

In the past, a number of analyses of the time series remote sensing products have been conducted for various applications. For example, the identification of crops and their growth seasons (Gillian *et al.*, 2007; Jakubauskas *et al.*, 2002; Zhang *et al.*, 2008), image processing (Lhermitte *et al.*, 2008), predicting the outputs and biomass of crops (Dash *et al.*, 2007; Weissteiner & Kuhbauch, 2005) and trend analysis (Hüttich *et al.*, 2007; Röder *et al.*, 2008a, 2008b). These studies used different methods which can be grouped into two classes: time domain analysis and frequency domain analysis. The main methods in time domain analysis are linear regression and statistical modeling. Linear regression is the most frequent method used to analyze the linear relationship of the variables with the corresponding times. From these results we can derive the linear trend of the variables and achieve predictions (Hüttich *et al.*, 2007; Röder *et al.*, 2008; Wardlow *et al.*, 2007; Weissteiner & Kuhbauch, 2005); Statistical model which is built by the mathematic theories is the alternative method to analyze the long time series in the time domain, and this method mainly

Received: 2008-11-06; **Accepted**: 2009-02-10

Foundation: National Key Basic Research Development Program (973) (No. 2007CB714407), National Natural Science Fund Project (No. 40640420073 and No. 40871163)

First author biography: JIANG Bo (1983—), female, graduate student studying quantitative remote sensing in the college of Geography and Remote Sensing Science in Beijing Normal University, E-mail: jiangboaj@163.com

depends on the characteristics of the original time series. We can also build models for prediction. However, this method has not been used very often in remote sensing, except the AutoRegression Integrated Moving Average (ARIMA) model (Alhamad *et al.*, 2007). The main methods that used in the frequency domain analysis of the time series are as follows. (1) Analysis with the harmonics of the time series, such as the Fourier analysis and the expanding method HANTs (harmonic analysis of time series). The principle of the Fourier analysis is to fit the spectrum of the original time series with a series of sine or cosine waves, whose magnitudes, phases and periods can be related to the phonology information (Canisius *et al.*, 2007; Jakubauskas *et al.*, 2001; Westra, 2007); (2) Wavelet analysis, whose principle is to use a base wavelet as a "window" to filter the original time series so that we can extract the different information corresponding to the different time frequencies. This method is often used for curve smoothing and removing the noises in a time series (Gillian *et al.*, 2007; Sakamoto *et al.*, 2006; Sakamoto *et al.*, 2005). Although these methods have been used in a variety of applications and resulted in some significant results, few have been used to predict the parameters in remote sensing. In this paper, we explore a method called Dynamic Harmonics Regression (DHR) to model and predict the LAI products. The details of the method in comparison with other methods have been explored in other study by the author (paper in writing), and it has been proved that DHR is a better method in predicting LAI.

The DHR method belongs to which analyzes the time series frequency domain analysis, and it is according to the characteristics of the spectrum of the original time series. This method has been used frequently in other fields, such as economics and engineering and other disciplines (Ng & Young, 1990; Pedregal & Trapero, 2007; Pedregal & Young, 2006; Taylor *et al.*, 2007). Since it has not been applied in remote sensing, we discuss the DHR method in analyzing the MODIS LAI time series products. In this study, we extract the trend and the seasonal components of the original LAI time series, model the dynamics of the LAI time series, and predict short-time LAI on the pixel basis.

2 METHOD

2.1 Dynamic Harmonics Regression (DHR)

2.1.1 Expression of each component in a time series

We usually apply an Unobserved Component (UC) model to express a time series, as follows (Young *et al.*, 1999):

$$y_t = T_t + C_t + S_t + e_t \qquad e_t \sim N(0,\sigma^2) \tag{1}$$

where y_t is the original value in time t; T_t is the trend component of the original time series; C_t and S_t are the period components, and S_t is the seasonal component, while C_t always has a longer cycle than S_t, the difference between which two is the time length; e_t is the residuals, which is always regarded as Gaussian white noise for convenience. UC model is used to model some components that can not be observed directly in a time series, such as the T_t, C_t and S_t in Eq. (1). There are a variety of types of UC models, and the DHR model can be regarded as a special one (Young *et al.*, 1999).

The DHR model is always used to fit three main components in a time series: which are T_t, S_t and e_t (C_t can be expressed as the same as S_t). The main feature of the DHR model is the expressions of seasonal or periodic components, so it is suitable for analyzing the time series with the remarkable seasonal variations. In the DHR model, the analysis of seasonal or periodic component is similar to the Fourier analysis, as expressed below:

$$S_t + e_t = \sum_{j=0}^{\left[\frac{s}{2}\right]} \left\{ a_{jt}\cos(\omega_j t) + b_{jt}\sin(\omega_j t) \right\} + e_t \qquad \text{where} \quad \omega_j = \frac{2\pi j}{s} \qquad j = 1,2,\cdots,\left[\frac{s}{2}\right] \tag{2}$$

where s is the length of a cycle. According to the theories of Fourier analysis, the number of harmonics of a time series is at most half of the seasonal cycle length. However, the difference between DHR and the general Fourier analysis is the expressions of the coefficients a_{jt} and b_{jt} in Eq. (2). In DHR, these coefficients are modeled with a dynamic model which makes the whole model "dynamic." Meanwhile, when modeling the trend component T_t in DHR, the dynamic model is also used and the trend is also "dynamic". These variables, which are dynamics with the time are all called Time Variable Parameters (TVP), and more details of the dynamic model used in DHR are described in the next section.

2.1.2 SS and GRW model

Many models have the dynamic function in mathematics, and the frequently used model is the State-Space (SS) model. The SS model is generally composed with 2 equations: the state equation and the observations equation. The model expresses the relation between the state values and the observations at every time (Young *et al.*, 2007), as follows:

$$\begin{aligned} &\text{state}-\text{equation}: \boldsymbol{x}_t = \boldsymbol{F}\boldsymbol{x}_{t-1} + \boldsymbol{G}\boldsymbol{\eta}_{t-1} \\ &\text{observation}-\text{equation}: \boldsymbol{y}_t = \boldsymbol{H}_t\boldsymbol{x}_t + \boldsymbol{e}_t \end{aligned} \tag{3}$$

where $\boldsymbol{x}_t$ is the state vector in time t; $\boldsymbol{\eta}$ expresses the system disturbing; $\boldsymbol{y}_t$ is the observations in time t; and $\boldsymbol{e}_t$ is the measuring errors which are regarded as the Gaussian distribution for convenience. The coefficients $\boldsymbol{F}$, $\boldsymbol{G}$ and $\boldsymbol{H}$ are the non-random known system matrices.

There are variable forms of the SS model, and the General Random Walk (GRW) models are used very often. The general expression of GRW models is:

$$\begin{pmatrix} x_{1t} \\ x_{2t} \end{pmatrix} = \begin{pmatrix} \alpha & \beta \\ 0 & \gamma \end{pmatrix} \begin{pmatrix} x_{1t-1} \\ x_{2t-1} \end{pmatrix} + \begin{pmatrix} \eta_{1t} \\ \eta_{2t} \end{pmatrix} \qquad Y_t = \begin{pmatrix} 1 & 0 \end{pmatrix} \begin{pmatrix} x_{1t} \\ x_{2t} \end{pmatrix} \tag{4}$$

where each variable in Eq. (4) expresses the vector of state value at time t (such as x_{1t}) and its errors (such as x_{2t}); $\boldsymbol{Y}_t$ is the observations at time t and we can regard it as each component

in a time series as in Eq. (1); the matrix $\begin{pmatrix} \alpha & \beta \\ 0 & \gamma \end{pmatrix}$ correspond to $\boldsymbol{F}$ in Eq. (3), and the matrices $\begin{pmatrix} \eta_{1t} \\ \eta_{2t} \end{pmatrix}$ and (1 0) correspond to $\boldsymbol{G}$, $\boldsymbol{H}$ in Eq. (3), respectively. Here $\boldsymbol{H}$ is defined, so if we define α、β、γ with the different values in Eq. (4), we can get the different $\boldsymbol{F}$ and $\boldsymbol{G}$, which can be used to express the different change situations. The typical cases include the Random Walk (RW: α=1, β=0, η_{2t}=0); the Integrated Random Walk (IRW: 0<α<1, β=γ=0, η_{2t}=0); the Local Linear Trend (LLT: η_{1t} =0); and the Damped Trend (α=β=γ=1, 0<γ<1). According to the experiences of Young (1989), the IRW model is suitable to express the situation which changes slowly, while the RW model is often applied to a quickly changing situation.

From the description in Section 2.1.1, we know that the DHR model uses the dynamic models (GRW models) to model each component in a time series. The choice of GRW models is a subjective process in practice, and in this paper we choose the IRW model to model the trend component, and the RW model to model the seasonal component according to the experience of Young as described above.

2.1.3 Estimating each component in a time series

The GRW models have been chosen to model the T_t and S_t components in a time series, and the estimations of these models are done with Kalman Filter (KF)/Fixed Interval Smoothing (FIS). Each step of estimating is composed of prediction and modification, so the DHR model can process the time series with missing data and outliers.

In order to compute conveniently, there are some parameters in the DHR model that have to be redefined, such as the Noise Variance Ration (NVR) Q_r and $\hat{p}_t$, where Q_r stands for the normalized matrix of variance and covariance of the system disturbing, and $\hat{p}_t$ is the covariance matrix of the estimations in the DHR models when filtering. In these parameters, the NVR can be regarded as the filter window, because the different NVR values determine the cut-off frequencies in the lower filter. Moreover, there are still some unknown parameters in the GRW models that are used to model each component, such as α、β、γ and η, which are all called the hyper-parameters. The NVR and these hyper-parameters determine the results of the filter together, and we need to ascertain them before estimating each component in a time series. There have been some methods for estimating the NVR and these hyper-parameters (Young *et al.*, 2007), and we choose the frequency domain estimation method in this paper. This method is generally concerned with approximating the theoretical pseudo-spectrum of the model (a function of the hyper-parameters in question) to the empirical pseudo-spectrum obtained directly from the time series, and we often implement the estimation and yield the optimal least squares fit to the empirically estimated spectrum. In addition, the empirical pseudo-spectrum is always the AutoRegression (AR) or periodic spectrum.

2.2 Implementation of the DHR model

The DHR model is implemented in the Captain Toolbox, which is developed on the MATLAB software platform by Young from Lancaster University (http://www.es.lancs.ac.uk/cres/captain). So in this paper, we do all the analysis based on the Captain Toolbox.

Although the DHR model has been used frequently in other applications, there are still some remarkable differences when applied to the MODIS LAI product. The main difference is that we use DHR model to model LAI products based on each pixel in the study regions, so we can not choose the parameters that the model needs subjectively. We therefore made some modifications when applying the DHR model to LAI products, and the ultimate goal is that it can process the LAI time series of each pixel automatically. The steps of applying the DHR model in this paper are as follows:

(1) Estimating the empirically spectrums of the original MODIS LAI time series. The LAI time series of different pixels around the globe may have the different lengths of period. According to the characteristics of the LAI time series, we choose 1a as the main period for all the LAI time series for convenience, so if 46 (samples/a) is the number of observations in a period, then there are at most 23 harmonics in a LAI time series defined in the Fourier analysis. In this paper, we use the AR spectrum as the empirical spectrum of each LAI original time series, and the order of it is defined as 46, indicating that 1a is the longest correlating time in a MODIS LAI time series.

(2) Based on the characteristics of the empirical spectrum or other a priori knowledge of the LAI original time series, we choose the main harmonics of the empirical spectrum to express the whole LAI time series.

(3) Estimation of the NVR and hyper-parameters with frequency domain method as described in Section 2.1.3.

(4) Using the estimated NVR and hyper-parameters in step (3) to estimate each component in the time series by KF/FIS, and predict the LAI values with the fitting model.

Step (2) described above is very subjective, since there is no rules to determine which harmonics are the most important. In other applications, the selection of harmonics is always based on the known noise power (Pedregal & Trapero, 2007), but that method can not be used in this study. As we all known, the products in remote sensing are easily affected by the environment, algorithms, clouds and many other factors, and these sources of noises are hard to ascertain, and the powers of these noises are difficult to get. So We loop steps (2), (3) and (4) in practice, and put the harmonics which are ordered by their powers into the model building one after another, and the estimated NVR and hyper-parameters each time are used to build the different DHR models and predict the LAI values with this model for the next year. When the correlations between the predicted LAI values and the mean LAI values in the previous year do not increase significantly any more, the harmonics are

ascertained and used to build the final DHR models. From a large number of experiments, we found that when the changes between the continuous correlations are smaller than 0.005 for at least two times, the harmonics can be ascertained. Furthermore, because the DHR model is built on the mathematical theories, the values predicted by the model may be negatives some times which are not valid for LAI. We need to replace them with the means of LAI in the previous years.

3 RESULTS

3.1 Decompose LAI time series

Each time series can be defined as the addition of the different components by the principle of DHR model (Eq. (1)), such as the trend, season component and so on. If we define the different parameters in the model we will get the different component, which is one of the main functions of the DHR model – time series decomposition. The interannual trend of LAI is very important. There are some methods, such as the linear regression, often used to fit the interannual and linear trend of a time series but they are not always very effective. However, the trend that is decomposed with the DHR model may be not always linear with the time because of the dynamic model (GRW).

Fig. 1 presents the LAI time series of an evergreen forest pixel. It has a remarkable increasing trend. Fig. 2 has three plots for the trend (a), the seasonal (b) and the residuals (c) component of the LAI time series. The trend in Fig. 2(a) is an obvious increasing curve, and it changes with the time; Fig. 2(b) shows the seasonal component which not only has the similar shape in each period but also changes with the time; and the residuals of Fig. 2(c) look very similar to the distribution of white noises, which proves that the primary information of the LAI time series have been gained adequately with the DHR model.

Fig. 2 proves that the DHR model is very effective for decomposing the time series, and the extracting trend is quite reasonable. That is because the DHR model uses the GRW dynamic models to model each component so that the fitting components are dynamic and characterize the whole original time series thoroughly.

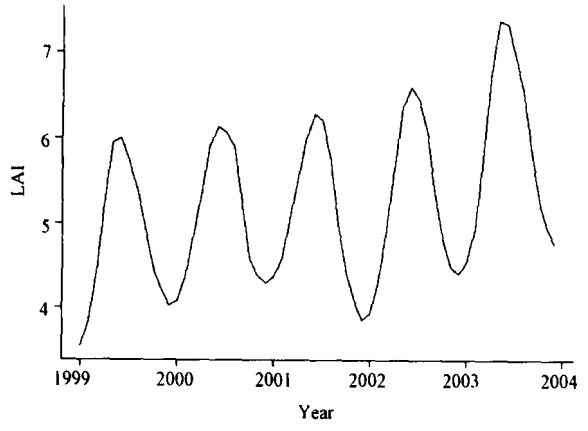

Fig. 1 LAI time series from 1999 to 2004

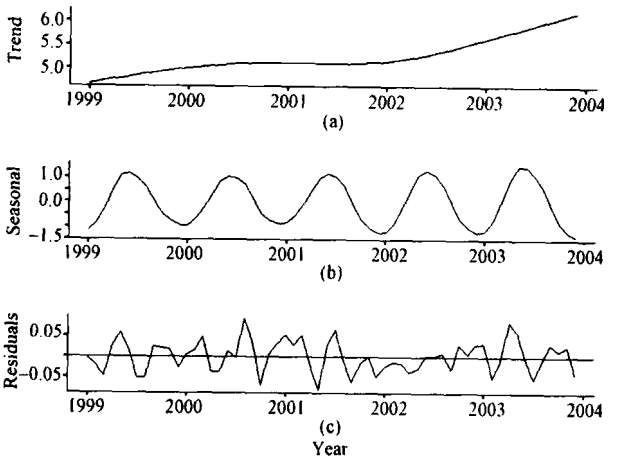

Fig. 2 Each component of the LAI time series that is decomposed with DHR model
(a) Trend component; (b) Seasonal component; (c) Residuals

3.2 Modeling results with DHR

The data we used in this study are MODIS LAI products of version 5 from the FLUXNET websites. The data includes 896 observation sites around the northern hemisphere. Because the original MODIS LAI products always have missing values, we used a method to fill in the missing data firstly (Fang *et al.*, 2008), so that the data we analyzed finally is continuous with no-gaps. The spatial resolution of the LAI product is 1km, temporal resolution is 8d (46 samples/a), and ranging from year 2001 to 2007. In order to explore the predicting ability of the DHR model for the LAI time series, we classified these sites into 9 land cover types: cropland and vegetation mosaic, croplands, deciduous forest, evergreen forest, mixed forest, grasslands, savannas, shrublands, and urban and built-up. We used the LAI data from year 2001 to 2006 to build the DHR model, and predicted the LAI values in 2007, and then compared the predictions with the original 2007 LAI values. The performances for each land covers are characterized by two statistical indices: root mean square error (RMSE) and correlation coefficient (R^2). Fig. 3 shows the results of the prediction R^2 of some cover types, and Table 1 shows the RMSE results of the prediction with the minimum, 25% quartile, medium, 75% quartile and maximum for each land cover types.

In order to analyze adequately, we also made a statistic of the prediction R^2 of each land cover type, and computed the correlations between the original LAI in 2001—2006 and the original LAI in 2007, and then got the correlations (CR) between them, which can be used to explain the relationship between the qualities of original data and the prediction precisions.

The results in Table 1 show that there are different prediction results when using DHR for different land cover types, such as croplands, deciduous forest, grasslands and shrublands. If the prediction errors are small it means the predictions are similar to the original values. When we check the prediction R^2 (not all are listed in this paper) of all land cover types, we can conclude that 5 land cover types - croplands and vege-

Table 1 Prediction RMSE of DHR model

Class name	Minimum	25% quartile	Median	75% quartile	Maximum
Croplands and vegetation mosaic	0.095	0.2405	0.343	0.544	1.188
Croplands	0.094	0.224	0.311	0.428	1.23
Deciduous forest	0.07	0.542	0.645	0.819	1.162
Evergreen forest	0.14	0.419	0.663	1.298	2.702
Grasslands	0.043	0.098	0.142	0.237	0.864
Mixed forest	0.185	0.552	0.679	0.826	1.374
Savannas	0.118	0.259	0.382	0.522	1.348
Shrublands	0.049	0.088	0.146	0.219	0.703
Urban and built-up	0.066	0.2	0.302	0.405	0.623

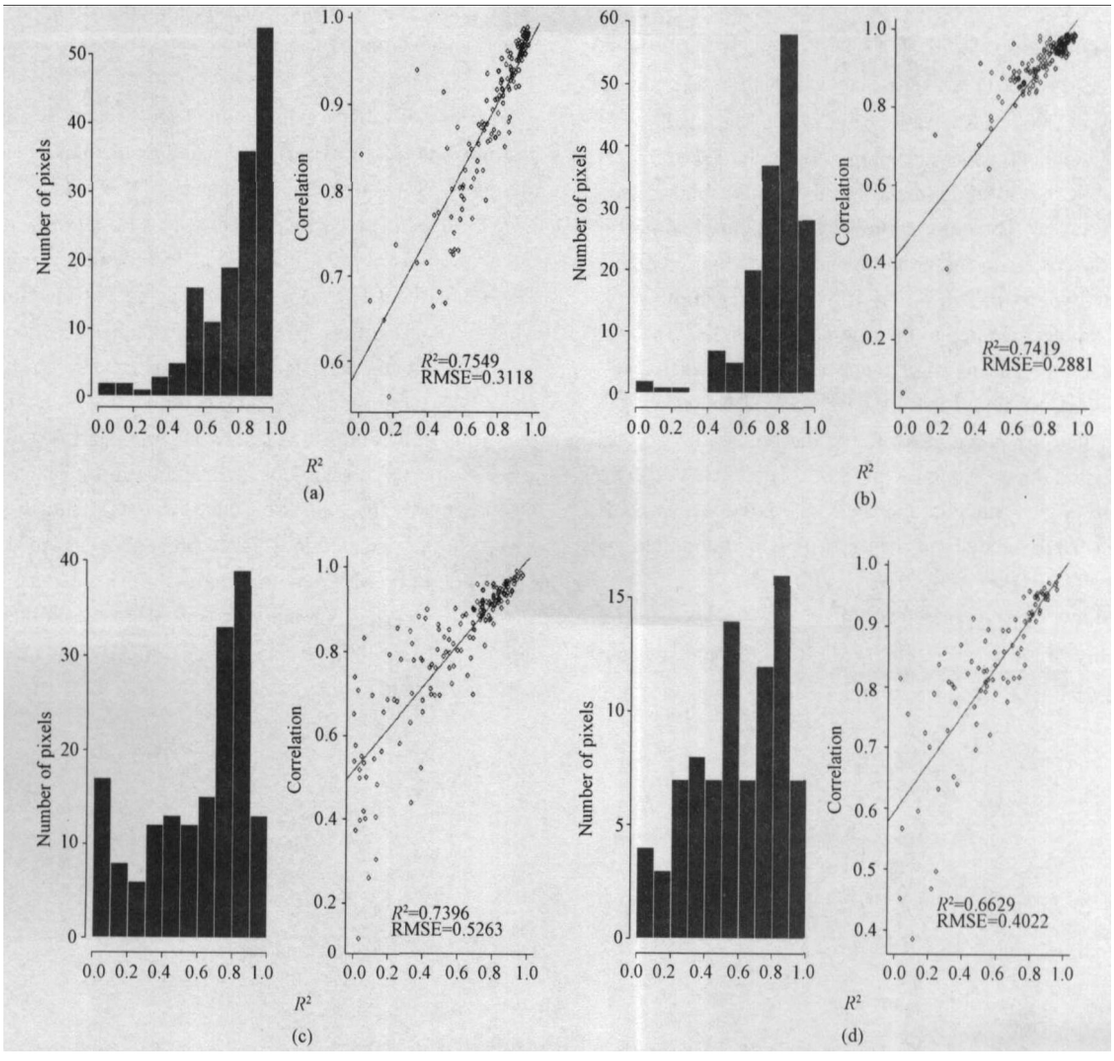

Fig. 3 Histograms of prediction R^2, and the R^2 of correlations of LAI in 2007 with the mean LAI in 2001—2006 and the prediction R^2 of some land cover types

(a) Croplands; (b) Mixed forest; (c) Evergreen forest; (d) Savannas

tation mosaic, croplands, deciduous forest, mixed forest and urban and built-up have the better LAI predictions, and the prediction R^2 of them are mostly larger than 0.6. The CRs are mostly high, indicating that the qualities of the original LAI time series in these types have the positive and nearly linear correlations with the predictions. While for other land cover types, such as evergreen forest, grasslands, shrublands and savannas, the DHR model did not predict well. The prediction R^2 of them are mostly below 0.5, and the CRs are not high either. Fig. 3 shows 4 land cover types to consolidate the conclusion. We can see clearly from the figure that croplands and mixed forest are of the good prediction results with the linear CRs larger than 0.7, but the predictions of grasslands and shrublands, are not good with low CRs.

In short, the prediction results are variable with different land cover types when using DHR models, and the qualities of the original data will affect the predictions. The details of the effectiveness of different factors to the DHR models prediction are described as follows.

3.2.1 Seasonality

From the conclusions above, we know that the more remarkable seasonal variation a land cover type has, the better prediction results when using the DHR model. These cover types include croplands and vegetation mosaics, croplands, deciduous forest and mixed forest. The evergreen forest type has the worse prediction results because it does not have the remarkable seasonal change. Fig. 4 and Fig. 5 show two examples.

Fig. 4 shows a pixel with good predictions, whose original LAI time series (2001—2007) is showed in Fig. 4(a) and the predictions in 2007 is showed in Fig. 4(b). The pixel corresponds to cropland and vegetation mosaic land cover. The original LAI curve is smooth, and has the remarkable seasonal change every year. The correlation between the original LAI in 2007 and the means in the previous years is as high as 0.975; the predicted values in 2007 (Fig. 4(b)) are lower in the growing period when compared to the original LAI in 2007, but still very close to the means of the previous years (2001-2007). From Fig. 4(a), we found that the original LAI values in 2007 are higher than the previous years, so the predictions are still reasonable, and the prediction R^2 is 0.955. The prediction curve in Fig. 4(b) is very smooth, and the shape is very reasonable, because the DHR model has removed most of the noises and disturbing effects.

Fig. 5 shows an evergreen forest pixel, Fig. 5(a) is the original LAI curve (2001—2007) and Fig. 5(b) compares the prediction curve in 2007 and the original values. From Fig. 5(a), we can see that the original LAI curve does not have the remarkable seasonal changes, and is affected much by the noises. It has some outliers, and the CR is just 0.856. The prediction curve has large difference with the original LAI, and there are 3 growing peaks in the prediction curve which may be affected by the indistinctive seasonal changes and the noises, as a result the prediction R^2 is just 0.249.

From the cases in Fig. 4 and Fig. 5, we demonstrate that the prediction results are variable according to the seasonal significances in a time series, and the DHR model is more appropriate to model the time series with the remarkable seasonal variation. When the requirement is met, the shape of the prediction curve will be very similar to the original time series. But if the time series does not meet the conditions, the prediction curve sometimes can be wrong.

3.2.2 Noises

Because of different disturbing factors, such as clouds, the satellite data are always affected much by the noises, and so are the MODIS LAI products. Because DHR model uses the KF/FIS to estimate each component in a time series, it can get rid of the noises when building and predicting a time series. Therefore, the DHR model is applicable for the time series which contains noises. And from the examples described above, we can see that the DHR model indeed predicts the smoother curve than the original one. Fig. 6 shows two examples to explain this point. Fig. 6(a) shows an original LAI time series curve from 2001 to 2007 of a deciduous forest pixel, and Fig. 6(b) compares the prediction curve in 2007 with the original curve and the mean values in the previous years of this pixel. From Fig. 6(a), we know that the pixel has a remarkable seasonality, but because of data acquisition and some other reasons, the original LAI time series is affected much during the growth period. The CR of this pixel is 0.888. Fig. 6(b) shows a very

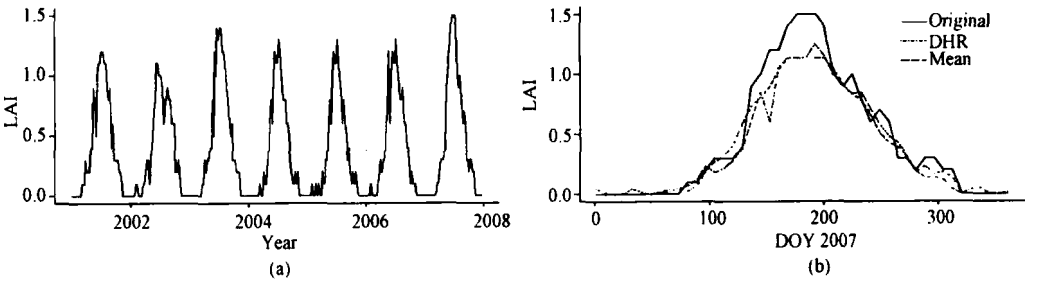

Fig. 4 Prediction results of two pixels of two classes

(a) Cropland and vegetation mosaic LAI original time series 2001-2007; (b) Prediction values of this pixel in 2007 comparing to the original LAI in 2007

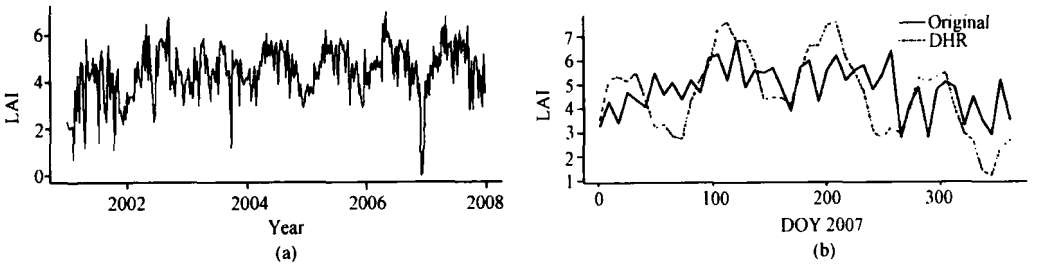

Fig. 5 Evergreen forest pixel prediction results

(a) LAI original time series of this pixel from 2001 to 2007; (b) Prediction values in 2007 comparing to the original LAI data

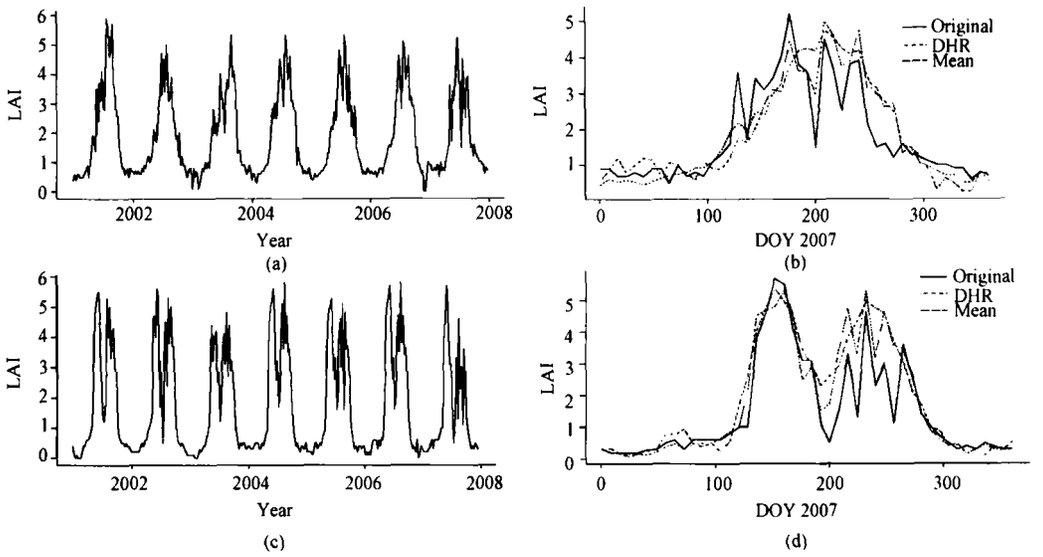

Fig. 6 Prediction results of two pixels belong to two classes

(a) LAI original time series from 2001 to 2007 of a deciduous forest pixel; (b) LAI prediction values of this pixel in 2007 comparing to its original data; (c) LAI original time series 2001—2007 of a mixed forest pixel; (d) LAI prediction values of this pixel in 2007 comparing to its original data

smooth prediction curve of the pixel which filters almost all the noises and disturbance, and the DHR predicts an exact shape of the LAI curve to the original one. However, the original LAI values in 2007 are affected much by noises, the prediction R^2 is just 0.676. Fig. 6(c) and Fig. 6(d) show another pixel. Fig. 6(c) is the original LAI curve from 2001 to 2007 of a pixel of mixed forest, and the time series has two remarkable seasons. But the pixel is also affected very much during the growth period, so the original LAI curve is not very smooth, and the CR is 0.919. Fig. 6(d) shows the prediction curve of this pixel in 2007 and the comparisons with the original curve and the mean values. The prediction curve has two significant seasonal growth periods which match the original ones (Fig. 6(c)), and it smoothes the curve. The prediction values are close to the means of the previous years, but the prediction R^2 is not high (0.772) because of the disturbance in the second growth period.

From the two examples in Fig. 6, we conclude that if a time series is not smooth because of the noises, disturbance or outliers but has a significant seasonality, the DHR model can predict very smooth curve reasonably. Although the prediction shape has some differences to the original curve, the prediction curve is more natural and reasonable. We can say that the prediction sometimes has better results than the original time series.

3.2.3 Filling data

Because the MODIS LAI products always have missing data, we filled the missing data using a published method (Fang *et al.*, 2008). But sometimes the filling data are mostly constant because the products have too many missing data, so the original LAI curve is not sound. When we use the DHR model to process these time series, the prediction results are always poor. For these 9 land cover types that we analyzed, shrublands, grasslands and savannas have many pixels with constant filling data, and the LAI ranges of them are usually not large, so the predictions are not very good. Fig. 7 shows two examples, and Fig. 7(a) and Fig. 7(b) show the results of a grasslands pixel, and Fig. 7(c) and Fig. 7(d) are the results of a savannas pixel. The original LAI values of these two pixels are all nearly below 1.0, and there are many lines and many constant filling data. The CRs of the two pixels are 0.931 and 0.947 respectively, which means that the growth situations of the two pixels are similar to the previous years. Fig. 7(b) and Fig. 7(d) are the prediction curves of the two pixels, which are smooth and more reasonable than the original curves. But the prediction values are lower than the original LAI data that may be affected by noises, so the prediction R^2 are just 0.861 and 0.824 respectively. This example also explains that the prediction R^2 are easily affected by the differences of the curve shapes.

Fig. 7 shows that if a time series has too many filling data, but a remarkable seasonal pattern, the DHR model can also get a more smooth and reasonable prediction curve than the original one. The DHR model has the ability to improve the MODIS LAI products.

3.3 Fitting the missing data with DHR model

The DHR model uses the KF/FIS to estimate each component and fit the missing data in the time series directly as long as the missing data are not too many. In order to explore this function of DHR, we choose two pixels as examples.

Fig. 8 shows two pixels, one is deciduous forest and the other is cropland. Fig. 8(a) shows the time series of the deciduous forest pixel, and we dropped 20 LAI data artificially to make a missing data series; Fig. 8(b) shows the fitting data of the pixel and the fitting residuals. In this plot, the red dash stands for the missing data, and green curve expresses the original LAI, and the yellow curve expresses the residuals between the fitting data and the original data. From Fig. 8(b) we can see clearly that the fitting data by using the DHR model is very close to the original data, and the fitting R^2 is 0.8344, the

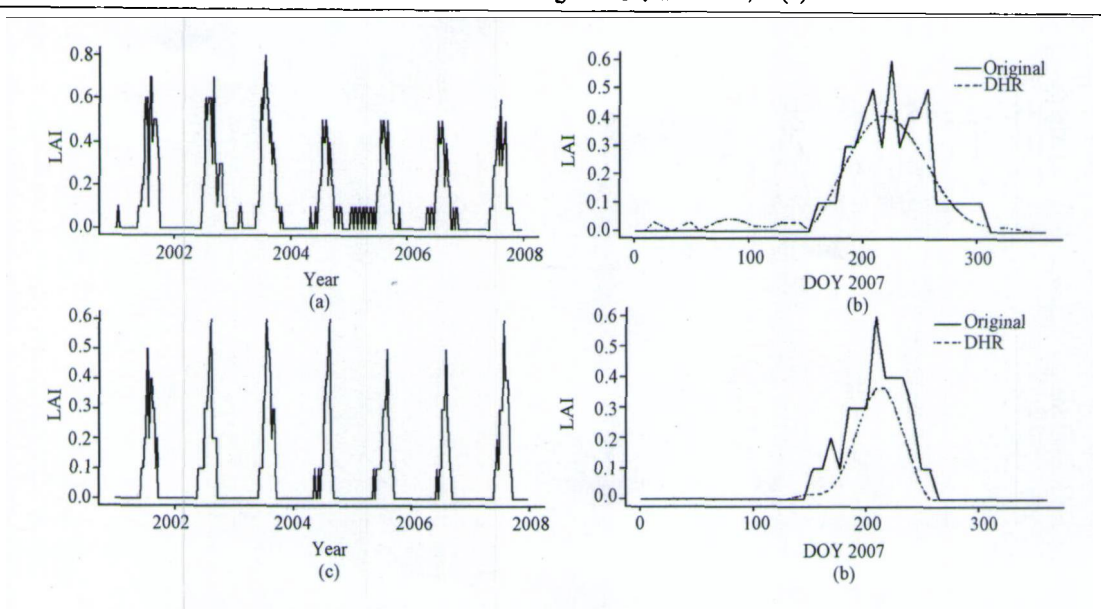

Fig. 7 Prediction results of the LAI time series with the filling data of two pixels

(a) LAI original time series from 2001 to 2007 of a grasslands pixel; (b) Prediction LAI values in 2007 comparing to the original data of this pixel; (c) LAI original time series from 2001 to 2007 of a shrublands pixel; (d) Prediction LAI values in 2007 comparing to the original data of this pixel

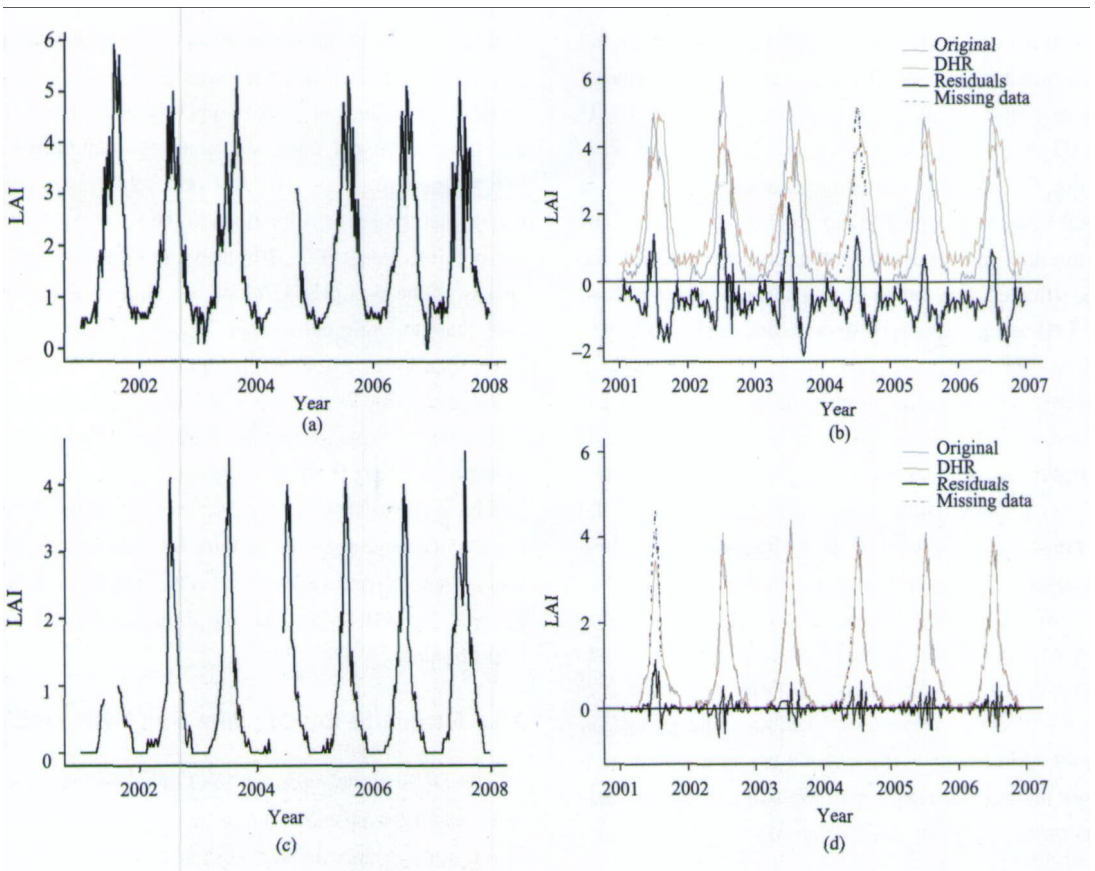

Fig. 8 Fitting the LAI time series with missing data using the DHR model

(a) LAI time series from 2001 to 2007 with a section of missing data of a pixel of deciduous forest; (b) Fitting the LAI time series 2001—2007 of this pixel; (c) LAI time series 2001—2007 with 2 section of missing data of a croplands pixel; (d) Fitting the LAI time series 2001—2007 of this pixel

RMSE is 0.9306, and the other data in the time series which does not have the missing data are also fitted very well, and the R^2 as high as 0.9376, RMSE is 0.9305. Fig. 8(c) shows the croplands pixel LAI curve with missing two parts of 20 data. The fitting results are showed in Fig. 8(d). The missing parts have been fitted very well, and the fitting R^2 is 0.9565, the RMSE is 0.5338. In addition, the whole fitting data in the 6 years are smoother than the original data, the residuals of fitting are very small, and the whole data fitting R^2 is 0.9401, the RMSE is 0.129. It has been proved that the DHR model has a good fitting function when the original data has good qualities and some missing data. And what's more, the fitting ability has no relation with the locations of missing data, which also proves that the DHR model has a good applicability.

4 CONCLUSION

The DHR model is based on the UC model and each component of the time series in DHR is expressed with the SS (State-Space) models. The season component is similar to the Fourier analysis, but each coefficient is expressed with the dynamic GRW model, which is one type of the SS models. We estimate the hyper-parameters and the filtering window NVR which are needed in the DHR model according to the characteristics of the spectrum of the original time series, and estimate each component and predict by using KF/FIS. In this paper, we analyzed the MODIS LAI time series products with the DHR model, and explore the applicability of DHR from three aspects: decomposition, prediction and fitting missing data.

Firstly, we explore the ability of main information extraction from a general time series with DHR, and the results have showned that the trend and the seasonal component are dynamic, and the residual component is similar to the distribution of the white noise. It proves that the DHR model can decompose the LAI time series effectively, and each extracted component is very reasonable, especially the trend component.

Secondly, we analyze the LAI time series with DHR, the data are from 896 sites all over the northern hemisphere with 9 land-cover types. The results show that although the prediction results are variable according to the land cover types or some special conditions, the DHR model is well suitable for remote sensing LAI product as a whole. When using DHR to predict, we need not know much information about the original time series at first, such as the length of period, the number of growth periods and so on, while we can build the model based on the characteristics of the spectrum of the original LAI time series. Some land cover types, such as croplands, deciduous forest, mixed forest and so on, which have the remarkable seasonal changes, can be predicted very well with DHR, and the prediction curves are usually more smooth and reasonable than the original ones.

Thirdly, we explore the fitting function of DHR for a time series with a few missing data. The examples in Section 3.3 proved that the fitting is very well when DHR is used in the time series of good qualities, and we need not know the number of missing data and the locations of them before fitting, DHR model is built just based on the spectrum of the original time series, and each component is estimated by KF/FIS. Both examples in Fig. 8 have good fitting R^2 larger than 0.8, and both of the whole time series have good fitting R^2 which are larger than 0.9. All of these examples demonstrate that DHR model is a valuable method in analyzing the time series which have a few missing data. The data in remote sensing always have missing data and outliers because of noises and other factors, so the DHR model is very suitable in analyzing remote sensing data.

However, there still remain some problems in this study. For example, we define the cycle period of all the pixels as 1a, which means the order of AR is 46 for all the pixels, but some land cover types do not have 1a as their significant growth period, so the parameters we defined here may not be completely reasonable. Further more, the method we use to ascertain the number of main harmonics to estimate the hyper-parameters and NVR needs to be explored further.

In short, this paper has demonstrated the useful applicability of the DHR model when used for the MODIS LAI time series products. We will continue our study to improve the DHR method for remote sensing data, and explore its applicability for other high-level remote sensing products.

Acknowledgements: Thanks to Mr. Ma Bin of Beijing Normal University for offering the pre-processed filtered MODIS LAI data.

REFERENCES

Alhamad M N, Stuth J and Vannucci M. 2007. Biophysical modelling and NDVI time series to project near-term forage supply: spectral analysis aided by wavelet denoising and ARIMA modelling. *International Journal of Remote Sensing*, **28**: 2513—2548

Canisius F, Turral H and Molden D. 2007. Fourier analysis of historical NOAA time series data to estimate bimodal agriculture. *International Journal of Remote Sensing*, **24**: 5503—5522

Dash J, Mathur A, Foody G M, Curran P J, Chipman J W and Lillesand T M. 2007. Land cover classfication using multi-temporal MERIS vegetation indices. *International Journal of Remote Sensing*, **28**(6): 1137—1159

Fang H, Liang S, Townshend J R and Dickinson R E. 2008. Spatially and temporally continuous LAI data sets based on an integrated filtering method: Examples from North America. *Remote Sensing of Environment*, **112**(1): 75—93

French A N, Schmugge T J, Ritchie J C, Hsu A, Jacob F and Ogawa K. 2008. Detecting land cover change at the Jornada experimental range, New Mexico with ASTER emissivities. *Remote Sensing of Environment*, **112**(4): 1730—1748

Galford G L, Mustard J F, Melillo J, Gendrin A, Cerri C C and Cerri C E P. 2008. Wavelet analysis of MODIS time series to detect expansion and intensification of row-crop agriculture in Brazil. *Remote Sensing of Environment*, **112**(2): 576—587

Hüttich C, Herold M, Schmullius C, Egorov V and Bartalev S A. 2007. Indicator of Northern Eurasia's land-cover change trends from SPOT-Vegetation time-series analysis 1998—2005. *International Journal of Remote Sensing*, **28**(18): 4199—4206

Jakubauskas M E, Legates D R and Kastens J H. 2001. Harmonic analysis of time-series AVHRR NDVI data. *Photogrammetric engineering and remote sensing*, **67**(4): 461—470

Jakubauskas M E, Legates D R and Kastens J H. 2002. Crop identification using harmonic analysis of time-series AVHRR NDVI data. *Computers and Electronics in Agriculture*, **37**(1-3): 127—139

Lhermitte S, Verbesselt J, Jonckheere I, Nackaerts K, van Aardt J A N, Verstraeten, W W and Coppin P. 2008. Hierarchical image segmentation based on similarity of NDVI time series. *Remote Sensing of Environment*, **112**(2): 506—521

Liu L and Xu H. 2007. The NDVI change rules of the main vegetations in HuangHe basin and the relationships with the meterologic factors. *Chinese Agriculture Meterology*, **28**(3): 334—337

Mao F, Hou Y, Tang S, Zhang J and Lu Z. 2007. Meadow classifying and dynamic changing studying in the Northern Tibetan based on the remote sensing data of 20 years. *Ecological applications*, **18**(8): 1745—1750

Ng C N and Young P C. 1990. Recursive estimation and forecasting of non-stationary time series. *Journal of Forecasting*, **9**(2): 173—204

Pedregal D J and Trapero J R. 2007. Electricity prices forecasting by automatic dynamic harmonic regression models. *Energy Conversion and Management*, **48**(5): 1710—1719

Pedregal D J and Young P C. 2006. Modulated cycles, an approach to modelling periodic components from rapidly sampled data. *International Journal of Forecasting*, **22**(1): 181—194

Röder A, Hill J, Duguy B, Alloza J A and Vallejo R. 2008a. Using long time series of Landsat data to monitor fire events and post-fire dynamics and identify driving factors. A case study in the Ayora region (eastern Spain). *Remote Sensing of Environment*, **112**(1): 259—273

Röder A, Udelhoven T, Hill J, del Barrio G and Tsiourlis G. 2008b. Trend analysis of Landsat-TM and-ETM+ imagery to monitor grazing impact in a rangeland ecosystem in Northern Greece. *Remote Sensing of Environment*, **112**(6): 2863—2875

Sakamoto T, Yokozawa M, Toritani H, Shibayama M, Ishitsuka N and Ohno H. 2005. A crop phenology detection method using time-series MODIS data. *Remote Sensing of Environment*, **96**(3-4): 366—374

Sakamoto T, Van Nguyen N, Ohno H, Ishitsuka N and Yokozawa M. 2006. Spatio–temporal distribution of rice phenology and cropping systems in the Mekong Delta with special reference to the seasonal water flow of the Mekong and Bassac rivers. *Remote Sensing of Environment*, **100**(1): 1—16

Taylor C J, Pedregal D J, Young P C and Tych W. 2007. Environmental time series analysis and forecasting with the Captain toolbox. *Environmental Modelling & Software*, **22**(6): 797—814

Wardlow B D, Egbert S L and Kastens J H. 2007. Analysis of time-series MODIS 250 m vegetation index data for crop classification in the US Central Great Plains. *Remote Sensing of Environment*, **108**(3): 290—310

Weissteiner C J and Kuhbauch W. 2005. Regional Yield Forecasts of Malting Barley (Hordeum vulgare L.) by NOAA-AVHRR Remote Sensing Data and Ancillary Data. *Journal of Agronomy and Crop Science*, **191**(4): 308—320

Westra T. 2007. Monitoring Sahelian floodplains using Fourier analysis of MODIS time-series data and artificial neural networks. *International Journal of Remote Sensing*, **28**(7): 1595—1610

Young P C, Pedregal D J and Tych W. 1999. Dynamic harmonic regression. *Journal of Forecasting*, **18**(6): 369—394

Young P C, Taylor C J, Tych W and Pedregal D J. 2007. The Captain Toolbox. Centre for Research on Environmental Systems and Statistics, Lancaster University, UK., Internet: www.es.lancs.ac.uk/cres/captain

Young P. 1989. Recursive estimation, forecasting and adaptive control. Control and Dynamic Systems, **30**, 119—166

Zhang M W, Qingbo Z, Zhongxin C, Jia L, Yong Z and Chong Fa C. 2008. Crop discrimination in Northern China with double cropping systems using Fourier analysis of time-series MODIS data. *International Journal of Applied Earth Observations and Geoinformation*, **10**(4): 476—485

Zhang X, Rui S, Bing Z and Tong Q X. 2008. Land cover classification of the North China Plain using MODIS_EVI time series. ISPRS Journal of Photogrammetry and Remote Sensing, **63**(4): 476—484

Zhao Y. 2003. Principles and Methods of Analyzing in Remote Sensing Applications. Beijing: Science Publisher

运用动态谐波回归模型对 MODIS 叶面积指数时间序列产品的分析与预测

江　波[1,2], 梁顺林[3], 王锦地[1,2], 肖志强[1,2]

1. 北京师范大学 地理学与遥感科学学院, 遥感科学国家重点实验室, 北京 100101;
2. 北京师范大学, 环境遥感与数字城市北京市重点实验室, 北京 100875;
3. 美国马里兰大学地理系

摘　要: 运用动态谐波回归模型(Dynamic Harmonic Regression, DHR)对 MODIS 的长时间序列的 LAI 产品进行分析, 可以从中分离出 LAI 随时间变化的多年趋势、季节变化及残差等主要成分, 通过建立的模型实现 LAI 年间变化的短时预测。本文将所述 DHR 模型分析方法试用于遥感数据产品随时间变化的信息提取, 对 LAI 年间变化的预测结果证明该方法用于遥感像元尺度 LAI 产品的时间序列分析与预测的效果良好。

关键词: 叶面积指数, 时间序列, MODIS, DHR 模型

中图分类号: TP702　　**文献标识码:** A

引用格式: 江 波, 梁顺林, 王锦地, 肖志强. 2010. 运用动态谐波回归模型对 MODIS 叶面积指数时间序列产品的分析与预测. 遥感学报, 14(1): 013—032
Jing B, Liang S L, Wang J D, Xiao Z Q. 2010. LAI time series analysis and prediction with Dynamic Harmonic Regression model. *Journal of Remote Sensing*, 14(1): 013—032

1 引　言

叶面积指数(LAI)是指每单位地表面积的植物叶面面积总量, 它对研究植物光合作用和能量交换是十分有意义的, 它与植被生态生理、叶片生物化学性质、蒸散、冠层光截获、地表净第一生产力等密切相关, 因此它是研究陆地生态系统一个十分重要的参数(赵英时, 2003)。从遥感学科发展至今, 已有从许多卫星遥感传感器, 例如 MODIS、SPOT、MERIS 等, 观测数据生成的 LAI 数据产品, 且因为卫星本身具有重访性的特点, 所以 LAI 等遥感产品已经积聚了一个长时间序列。对长时间序列的遥感产品, 如 LAI 等, 进行时间序列的分析, 可以从中提取出地表覆盖, 尤其是植被多年变化的趋势、季节变化等动态信息, 这些重要信息对于掌握和了解地表动态变化、气候影响等具有重要意义, 对遥感产品的长时间序列的分析成为现代遥感学科研究的重要方向之一, 其中一项是探讨有效的用于遥感产品的时间序列分析的方法。

MODIS 是中等分辨率星载传感器的简称, 它拥有 36 个波段, 从可见光到热红外, 其对地观测覆盖全球, 时间分辨率为 8d, 其 LAI 产品为 MOD15A2, 主要的空间分辨率为 500m 或 1km。由于 MODIS 数据本身的原因, 及云、天气、噪音等影响, 所得到的 LAI 产品在时间序列上常常具有数据缺失、噪音过多等特点, 因此需要研究可以从这些序列中提取出有用信息, 同时实现去噪、拟合、预测等功能的方法。

很多科学家和研究者对长时间序列的遥感产品进行了分析, 并且应用于不同的方面, 如农作物生长季节判断、分类(Gillian 等, 2007; Jakubauskas 等, 2002; Zhang 等, 2008); 地表覆盖变化及监测(Dash 等, 2007; French 等, 2007; Zhang 等, 2008);图像处理(Lhermitte 等, 2008); 作物产量及生物量预测(Alhamad 等, 2007; Weissteiner & Kuhbauch 2005)及

收稿日期: 2008-11-06; **修订日期:** 2009-02-10

基金项目: 国家重点基础研究发展计划(973 计划)项目(编号: 2007CB714407)和国家自然科学基金项目(编号: 40640420073, 40871163)。

第一作者简介: 江波(1983—), 女, 硕士研究生, 目前就读于北京师范大学地理学与遥感科学学院地图学与地理信息系统专业, 研究方向为定量遥感。E-mail: jiangboaj@163.com。

趋势分析(Hüttich 等, 2007; Röder 等, 2008a; 2008b; 毛飞等, 2007; 刘绿柳 & 许红梅, 2007)等。这些不同方面的时间序列分析, 运用多种方法, 主要可以划分为两大类: 时间域分析及频率域分析。时间域分析的主要方法是线性相关性分析及建模分析, 其中: (1)线性相关分析, 主要是运用研究对象值或其多年异常值与对应时刻的线性相关分析, 并可与温度、水分等各气候因子相关联分析, 从而得到多年主要的趋势变化, 实现预测等功能(Hüttich 等, 2007; Röder 等, 2008b; Wardlow 等, 2007; Weissteiner & Kuhbauch 2005; 毛飞等 2007; 刘绿柳 & 许红梅, 2007); (2)建模分析, 主要是针对时间序列本身的特点, 应用数学方法建立模型, 实现对该序列的拟合及预测功能, 目前这种方法在遥感中的应用并不普遍, 主要有 AugoRegression Intergrated Moving Average (ARIMA)模型(Alhamad 等, 2007)等。频率域分析的方法主要有: (1)谐波分析, 主要有傅里叶分析及后来发展的时间序列谐波分析(Harmonic Analysis of Time Series, HANTs)等。它的主要原理是用一系列正弦或余弦波近似拟合原始序列的波谱, 根据得到的拟合波的振幅、周期、相位角等分析得到该序列的相关物候等信息(Canisius 等, 2007; Jakubauskas 等, 2001; Westra 2007); (2)小波分析, 主要是用选中的母小波作为窗口在频率域对原始序列滤波, 可以提取出对应于不同时间分辨率的原始时间序列的信息, 且该方法多用于去噪平滑(Gillian 等, 2007; Sakamoto 等, 2006; Sakamoto 等, 2005)。虽然这些不同方法在不同方面的研究取得了一定的进展, 但目前并没有很好的方法用于遥感产品的预测, 因此本文主要研究了运用 DHR 方法对 LAI 时间序列的建模及预测, 另外本文作者也进行了 DHR 与其他时间序列方法的比较, 证明了 DHR 方法是其中一种较好的方法。

本文所探讨的运用动态谐波回归模型的方法也可划分在频率域方法类中, 主要根据原始序列在频率域的特点进行分析, 该方法在其他领域, 如经济学、工程学等方面有成熟地运用(Ng & Young 1990; Pedregal & Trapero 2007; Pedregal & Young 2006; Taylor 等, 2007), 但在遥感学科中还没有研究和应用。本文将该方法用于对 MODIS LAI 时间序列数据的分析, 实现了: (1)对 LAI 原始时间序列的趋势、季节变化等主要信息的提取; (2)拟合 LAI 时间序列; (3)实现对遥感像元尺度 LAI 年间变化特征的短时预测。

2 DHR 模型分析方法

2.1 DHR 模型

2.1.1 时间序列各成分表达

对于一个时间序列, 一般可以用 Unobserved Component(简称 UC)模型表达, UC 模型一般表示为(Young 等, 1999):

$$y_t = T_t + C_t + S_t + e_t \qquad e_t \sim N(0,\sigma^2) \tag{1}$$

式中, y_t表示原始时间序列在t时刻的值; T_t为原始序列在该时刻的趋势成分; C_t及 S_t表示原始序列在该时刻的周期成分, 其中 S_t为季节周期成分, C_t为比季节周期更长的周期, 两者只是周期长度的差异; e_t为残差, 通常为了简便, 视为高斯白噪音分布。UC 模型的含义为对不能直接观察到的成分拟合模型, 如在式(1)中, T_t、C_t及 S_t等分量是不能通过观察直接得到的。UC 模型有多种表现形式, DHR (Dynamic Harmonic Regession)模型可以认为是 UC 模型的一种特殊表现形式(Young 等, 1999), 它建立在 UC 模型的基础上。

DHR 模型主要用于拟合时间序列的 3 个成分, 即 T_t、S_t及 e_t, 其中由于周期成分 C_t与 S_t只是周期长度的区别, 因此用 S_t表示。DHR 模型的主要特点是对季节和周期成分的表示, 因此它主要适用于有季节或周期变化成分的时间序列分析, 对该成分的分析近似于傅里叶分析, 如式(2)所示:

$$S_t + e_t = \sum_{j=0}^{\left[\frac{s}{2}\right]} \left\{ a_{jt}\cos(\omega_j t) + b_{jt}\sin(\omega_j t) \right\} + e_t \tag{2}$$

$$\text{且} \qquad \omega_j = \frac{2\pi j}{s} \qquad j = 1,2,\cdots,\left[\frac{s}{2}\right]$$

式中, s 为序列长度, 根据傅里叶理论, 谐波个数最多只能为周期长度的一半。但与普通的傅里叶分析不同, DHR 选择由一种动态模型表示式中的系数 a_{jt}和 b_{jt}, 这种模型可随时间变化, 因此 DHR 拟合的季节成分实现了"动态"的功能。同样, 对于趋势成分 T_t 的拟合, DHR 也选择了这种动态模型, 也实现了"动态"的功能。这种动态模型在 2.1.2 节中有详细说明。在 DHR 中, 这种变量统称为 Time Variable Parameters(TVPs)。

2.1.2 SS 模型及 GRW 模型

在数学中具有"动态"功能的模型有多种, 其中最常用的一类为 SS 模型(State-Space), SS 模型一般由 2 个函数表达: 状态值方程和观察值方程, 它表达了每个时刻观测值和状态值的关系(Young 等, 2007):

$$\begin{aligned} &\text{state}-\text{equation}: \boldsymbol{x}_t = \boldsymbol{F}\boldsymbol{x}_{t-1} + \boldsymbol{G}\boldsymbol{\eta}_{t-1} \\ &\text{observation}-\text{equation}: \boldsymbol{y}_t = \boldsymbol{H}_t\boldsymbol{x}_t + \boldsymbol{e}_t \end{aligned} \tag{3}$$

式中, $\boldsymbol{x}_t$ 为 t 时刻的状态矢量; $\boldsymbol{\eta}$ 为系统扰动分量; $\boldsymbol{y}_t$ 是 t 时刻的随机观察量; e_t 为假定符合高斯分布的测量误差。式(3)中的 $\boldsymbol{F}$、$\boldsymbol{G}$ 和 $\boldsymbol{H}$ 视为已知的非随机的系统矩阵。

SS 模型也有多种表现形式, 其中最常用的一种为 GRW (General Random Walker)类模型, GRW 类模型包括多种形式, 其通用形式为:

$$\begin{aligned} &\begin{pmatrix} x_{1t} \\ x_{2t} \end{pmatrix} = \begin{pmatrix} \alpha & \beta \\ 0 & \gamma \end{pmatrix} \begin{pmatrix} x_{1t-1} \\ x_{2t-1} \end{pmatrix} + \begin{pmatrix} \eta_{1t} \\ \eta_{2t} \end{pmatrix} \\ &Y_t = \begin{pmatrix} 1 & 0 \end{pmatrix} \begin{pmatrix} x_{1t} \\ x_{2t} \end{pmatrix} \end{aligned} \tag{4}$$

式中, 每个变量表示为该时刻状态值(如 x_{1t})与其误差(如 x_{2t})的矢量形式; 式中 $\begin{pmatrix} \alpha & \beta \\ 0 & \gamma \end{pmatrix}$ 项对应于式(3)中的 $\boldsymbol{F}$ 矩阵, 同理 $\begin{pmatrix} \eta_{1t} \\ \eta_{2t} \end{pmatrix}$ 项和(1　0)项则分别对应于式(3)中的 $\boldsymbol{G}$、$\boldsymbol{H}$ 矩阵; $\boldsymbol{Y}_t$ 为 t 时刻的观测量, 即可认为是时间序列所对应的各成分。$\boldsymbol{H}$ 矩阵已确定, 则通过对 α、β、γ 和 η 分别取值, 即可得到确定的 $\boldsymbol{F}$、$\boldsymbol{G}$ 矩阵, 即可表示不同的变化情况, 其主要的取值方式有 Random Walk(RW)模型: α=1, β=γ=0, η_{2t}=0; Smoothed Random Walk(SRW)模型: 0<α<1, β=γ=0, η_{2t}=0; Integrated Random Walk(IRW)模型: α=β=γ=1, η_{1t}=0; Local Liner Trend(LLT)模型: α=β=1, 0<γ<1。根据已有的经验(Young, 1989)可知, IRW 模型适于表达缓慢变化的情况, RW 模型适于表达变化快速的情况。

根据 2.1.1 节的描述, 可知 DHR 模型对时间序列的各成分拟合选择了动态模型, 即为该节所介绍的 GRW 类模型。在实际应用中, 各成分根据每个 GRW 模型的特点可以有主观的选择。在本文的研究中, 对 MODIS LAI 时间序列中趋势变化成分的拟合选用了 IRW 模型, 而对季节变化成分选用 RW 模型拟合。

2.1.3　时间序列各成分估计

在 DHR 模型中, 对主要成分如 T_t、S_t 的拟合运用了 GRW 类模型, 实际各模型的估计由 Kalman Filter(KF)/Fixed Interval Smoothing(FIS)滤波实现, 每个步骤由预测–修改两步完成(Young 等, 1999), 因此对于有缺失数据及有异常值的时间序列, DHR 模型也能实现拟合。

为了更好地运用 KF/FIS 估计每个成分, DHR 模型在滤波过程中定义了参数的噪声方差比(Noise Variance Ratio, NVR) Q_r 及 $\hat{p}_t$, Q_r 表示系统扰动的归一化误差协方差矩阵, $\hat{p}_t$ 表示在滤波过程中状态估计量的误差协方差矩阵, 其中 NVR 可以视为滤波窗口, 不同的 NVR 确定了低通滤波的不同切断(cut-off)频率; 同时各成分表示时所选择的 GRW 过程模型中还存在一些未知的参数, 如未确定的 α、β、γ 及 η, 若将这些参数称为超参数, 则 NVR 和超参数就确定了滤波表现, 故在实现滤波估计各成分之前需要确定这些参数。在实际的应用中, NVR 和超参数的估计有多种方法(Young 等, 2007), 本文所选择的为频率域估计方法, 即使原始时间序列的自相关(AutoRegreesion, AR)或周期图波谱与拟合得到的波谱最接近, 通过最小二乘估计得到 NVR 及各超参数。

2.2　DHR 模型拟合方法的实现

DHR 模型建模是基于 MATLAB 平台开发的 Captain Toolbox 软件包, 该软件包由 Lancaster University 的 Young 等设计并发展(http://www.es.lancs.ac.uk/cres/captain)。因此本文主要基于 Captain Toolbox 软件包实现 DHR 模型的拟合。

运用 DHR 模型分析 MODIS LAI 的时间序列产品, 同该模型在其他领域的应用有着很大的区别, 其中最大的一个区别是在基于像元的基础上处理一个试验区域的 LAI 产品数据时, 不能每个像元点靠主观判断选择建模参数, 因此在具体应用中稍作改进, 实现自动处理每个像元点。本研究中 DHR 建模分为几个步骤实现:

(1) 估计 MODIS LAI 原始序列的经验波谱。由于研究的是不同像元点的 LAI 时间序列, 且覆盖全球, 因此不同的像元会有不同的周期表现, 针对地表 LAI 的季节变化特征, 选择 1a 作为所有像元点的主要变化周期。按照 MODIS 的 LAI 产品年采样数据量, 选择 46(样/a)为所有像元点周期的观察值个数, 按照谐波理论, 所有像元时间序列的谐波个数最多为 23 个。这里主要是用 LAI 数据原始时间序列的自回归(AR)波谱作为经验波谱, 且阶数为 46, 即对于该 MODIS LAI 时间序列, 1a 是最大相关的时间长度。

(2) 应用先验知识或原始时间序列波谱的特点, 选择主要的谐波表示要拟合的 LAI 时间序列变化成分。

(3) 应用 2.1.3 节中所描述的频率域方法估计 NVR 及超参数。

(4) 用第(3)步估计得到的 NVR 及其他超参数由 KF/FIS 实现每个成分的估计及预测功能。

上述第(2)步是一个很主观的过程，没有一个比较准确的准则判断哪几个谐波是最主要的，在已有的一些研究中主要是根据噪音水平选择主要谐波(Pedregal & Trapero, 2007)，但在本文的研究中并不适用，因为遥感产品可能由数据观测环境、产品算法等多种因素造成时间序列上的数据噪音，噪音源无法确定，噪音大小无法准确获知。因此在实际的应用中，我们将第(2)、(3)、(4)步反复循环执行，即根据原始序列的自回归波谱所得到的谐波按能量大小排列，依次加入 DHR 模型的拟合，每次得到的 NVR 及超参数用来建立不同的 DHR 模型并估计下一年的 LAI，与该点多年的 LAI 序列的平均值做相关分析，当相关系数不再连续增大，或者增大的幅度非常小时，确定谐波周期和个数即可确定该点的 DHR 模型。研究通过多次实验，最后根据经验判断，当预测 LAI 值与多年平均 LAI 值相关系数的增长幅度至少连续 2 次小于 0.005 时为不显著增大。另外，因为该模型是按照数学理念拟合，最后得出 LAI 有时会有负值，不符合逻辑，因此最后的结果若为负值，用该时刻的多年均值代替。

3 结果分析

3.1 DHR 模型分解 LAI 时间序列

根据 DHR 模型的原理，即每个时间序列数据是由不同周期成分加和得到，可以通过设定不同的参数，运用 KF/FIS 滤波得到不同的各成分，因此用 DHR 模型对时间序列分析，可以从原始序列中提取出趋势、季节变化等主要成分。LAI 多年趋势的变化信息对于很多研究非常重要，目前有的一些方法，主要是通过线性相关等方法拟合出趋势，而且很多拟合的趋势呈直线型，与实际情况趋势的多年变化是不符合的。DHR 模型分离出的趋势成分是随时间变化的曲线形式，因为它使用的 GRW 模型拟合，所以更合理。

图 1 显示了一个常绿林像元点的 LAI 时间序列。从图 1 看出，该序列是有明显的上升趋势，运用 DHR 模型分离出了季节、趋势、残差等成分，在图 2 中显示。图 2 的趋势成分明显为上升曲线，但不是简单的直线，而随时间变化；分离出的季节成分每个周期类似，但也随时间变化；分离出的残差基本符合白噪音分布，证明确实从原始序列中已经提取了该像元 LAI 变化特征中主要的信息。

从该例子证明，DHR 模型用于时间序列的分解是有效的，得到的趋势成分更合理，由于拟合各成分用的是 GRW 模型，因此拟合的各成分模型也是随时间变化，可以捕捉更完整的时间序列信息。

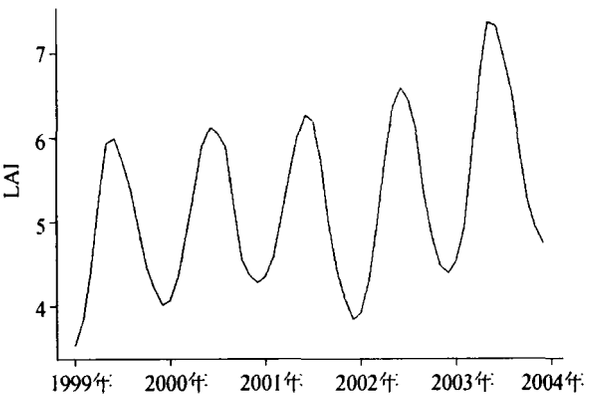

图 1 LAI 时间序列(1999—2004 年)

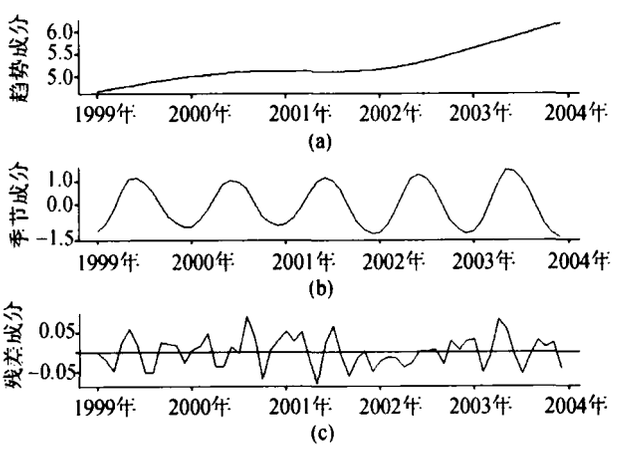

图 2 DHR 模型分离出各成分
(a) 趋势成分; (b) 季节成分; (c) 残差成分

3.2 DHR 模型预测效果

本研究所用数据为 MODIS 第 5 版的 LAI 产品，从 FLUXNET 网站下载全球 896 个观测站点的 LAI 时间序列数据。由于 MODIS 的 LAI 产品本身有缺失等问题，原始产品经过已有的一种补缺方法进行预处理(Fang 等, 2008)，得到完整数据。因此最后用于模型的是完整连续的 LAI 时间序列数据，时间范围 2001—2007 年，空间分辨率为 1km，时间分辨率为 8d(46 次/a)。为了更好地探讨 DHR 方法对不同情况下 LAI 预测的效果，将所有的站点像元归分为 9 地类，依次为：农作物与自然植被混合，农作物，落叶林，常绿林，混交林，草地，稀树草原，灌木林地，市内绿化区，分别采用 2001—2006 年的 6a LAI 数据建立 DHR 模型，并预测 2007 年 LAI 数据，最后得到的预测结果与原始 LAI 数据比较，按照均方根误差(RMSE)相关系数(R^2)两个统计量对各种地类分别统计，R^2 统计结果如图 3，RMSE 统计结果如表 1，表 1

表 1　DHR 模型预测结果 RMSE 精度

地类名称	最小值	1/4 分位值	中值	3/4 分位值	最大值
农作物与自然植被混合	0.095	0.2405	0.343	0.544	1.188
农作物	0.094	0.224	0.311	0.428	1.23
落叶林	0.07	0.542	0.645	0.819	1.162
常绿林	0.14	0.419	0.663	1.298	2.702
草地	0.043	0.098	0.142	0.237	0.864
混交林	0.185	0.552	0.679	0.826	1.374
稀树草原	0.118	0.259	0.382	0.522	1.348
灌木林	0.049	0.088	0.146	0.219	0.703
市内绿化区	0.066	0.2	0.302	0.405	0.623

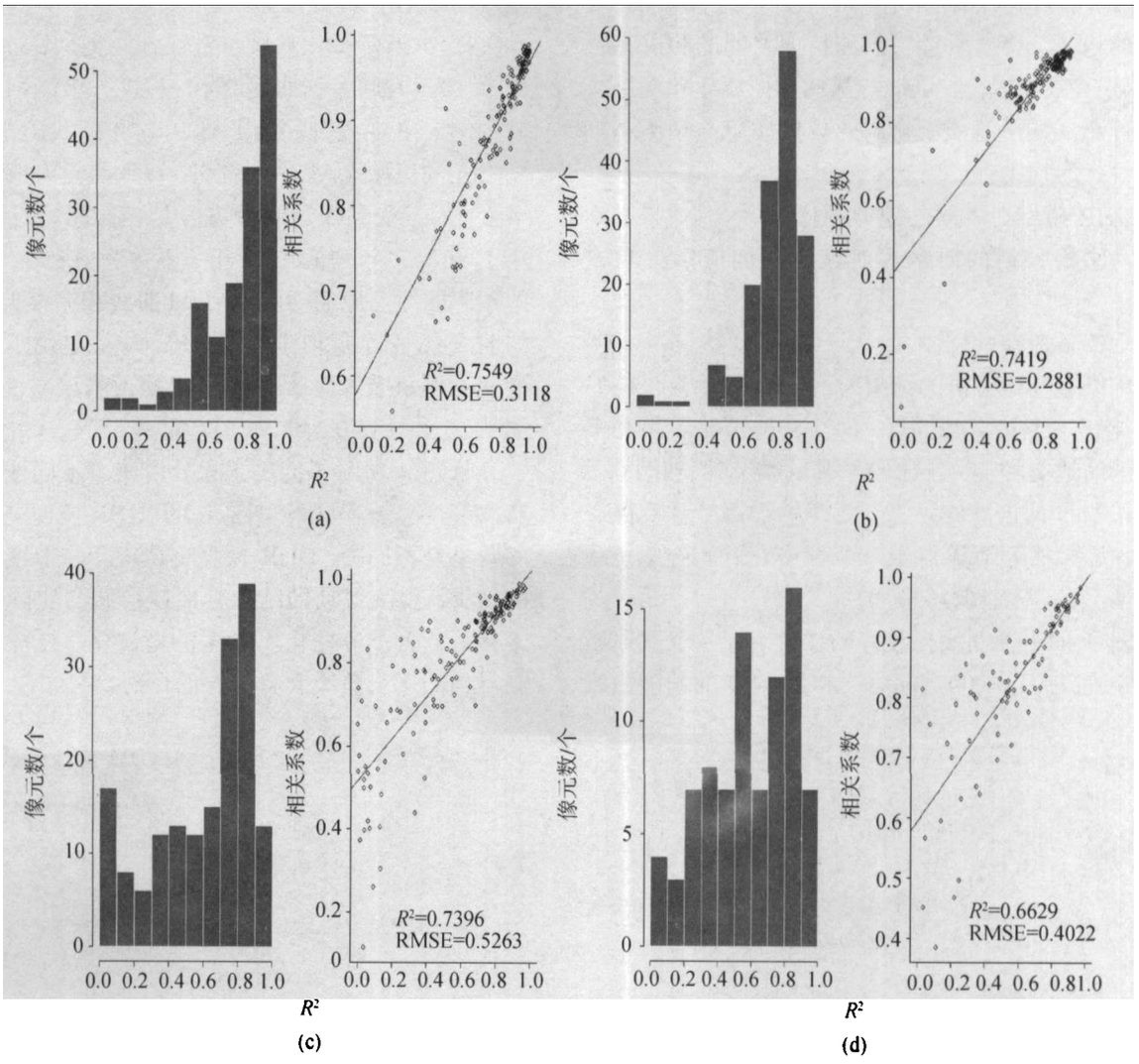

图 3　预测精度 R^2 直方图及各像元预测值与多年均值的相关系数与预测精度相关性

(a) 农作物; (b) 混交林; (c) 常绿林; (d) 稀树草原

列出了各地类预测精度 RMSE 的最小值、1/4 分位值、中值、3/4 分位值及最大值统计结果。

同时本文还统计了 9 地类的各自预测精度 R^2, 并计算了原始数据 2007 年的 LAI 值与前 6a LAI 均值的相关系数, 同时拟合了此相关系数与预测精度 R^2 之间的相关性, 主要为了说明数据质量与预测精度的关系。

表 1 统计结果表明了各地类用 DHR 模型预测, 效果是不同的, 有些地类如农作物、落叶林、草地和灌木林等, 误差范围比较小, 证明这些地类的预测值接近原始值; 常绿林地类的误差范围较大, 证明了预测值与原始值相差较大。从所有地类预测精度及数据质量的统计结果看(本文没有全部列出), 用 DHR 模型预测得到的结果中, 农作物与自然植被

混合、农作物、落叶林、混交林及市内绿化区这 5 类的 LAI 时间序列预测的效果最好，R^2 值在 0.6 以上的像元数占大多数，且这 5 类的预测精度与原始数据及均值相关系数的线性相关较好，证明了这 5 类原始数据的质量与预测结果有接近线性相关的关系；其他地类如常绿林、草地、稀树草原和灌木林，从得到的预测精度看，运用 DHR 模型做的预测并不很理想，R^2 在 0.5 以下的像元点所占比例也较高，而预测精度与原始数据及均值相关系数的散点图并不具有很好的线性相关。图 3 选择了 4 种地类加以说明，从图中明显看出，农作物、混交林属于预测精度较好的地类，数据质量与预测精度之间的相关性比较明显，在 0.7 以上；草地与稀树草原属于预测结果并不理想的两种地类，它们的数据质量与预测精度没有很好的相关性。

DHR 模型对不同的地类进行应用，其效果是不同的，原始数据的质量等对该方法的应用影响也较大。

3.2.1 季节显著性影响

从以上整体分析的结果看，DHR 预测效果较好的地类有一个共同的特点，即与其他预测效果并不很理想的地类相比，有比较显著的季节性变化特征，如农作物与自然植被混合、农作物、落叶林及混交林等，常绿林等地类由于季节性变化并不显著，预测效果不太理想(图 4、图 5)。

图 4 即为预测效果较好的 1 个像元点，其原始时间序列(2001—2007 年)曲线和 2007 年的预测曲线分别为图 4(a)、(b)。该像元点属于农作物与自然植被混合地类，从图 4(a)的原始序列看出，该像元点的 LAI 序列很平滑，且每年 LAI 变化情况类似，有明显的季节变化，其 2007 年的 LAI 与多年均值相关系数为 0.975；图 4(b)显示预测的曲线为 2007 年 LAI 与原始 LAI 及多年平均 LAI 的比较，在生长高峰期 LAI 值偏低，但与多年均值很接近，该像元点 2007 年 LAI 确实比前几年在生长高峰期要大，其预测精度 R^2 为 0.955。从图 4(b)看出预测曲线非常平滑，且主要的生长形状基本预测出，几乎滤掉了所有噪音造成的 LAI 值的跳动。

图 5 所示像元点属于常绿林地类，图 5(a)为其原始 LAI 时间序列曲线(2001—2007 年)，图 5(b)是其预测 LAI 曲线与原始 LAI 2007 年曲线的比较。从图 5(a)的原始 LAI 序列看出，该地类没有明显的季节变化，且受到噪音的影响很大，存在异常值，2007 年 LAI 与多年均值 LAI 相关系数为 0.856；图 5(b)的预测曲线与原始 2007 年 LAI 曲线相差很大，预测的曲线有 3 个近似于生长高峰，应该是由于季节性变化不明显及噪音影响所造成的预测误差，因此预测精度 R^2 只有 0.249。

从图 4 和图 5 的例子充分说明了不同地类由于其季节性显著程度不一样，运用 DHR 模型进行预测的效果是不同的，DHR 模型更适应于季节变化显著的地类，预测得到的结果其曲线形状与实际曲线非常接近，而季节变化不显著的情况下，往往可能预测得到的生长曲线会有错误的形态。

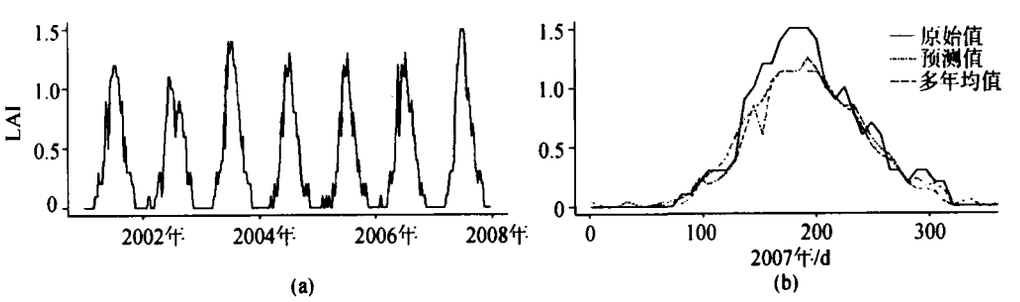

图 4 像元点预测结果

(a) 像元 LAI 原始时间序列 2001—2007 年; (b) 2007 年该像元点预测结果与原始序列比较

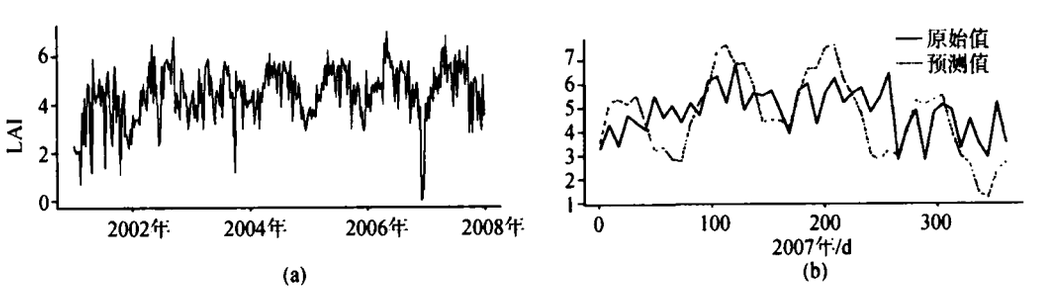

图 5 常绿林类像元预测结果

(a) LAI 原始时间序列 2001—2007 年; (b) 该像元点 2007 预测结果与原始数据比较

3.2.2　噪音影响

由于卫星数据获取本身的原因，如云等因素的影响，最后得到的遥感卫星数据产品往往会受噪音影响很大，MODIS 的 LAI 产品也存在受噪音影响较大的问题。DHR 模型运用于噪音影响较大的时间序列分析时，因为 DHR 模型用于预测时是采用 KF/FIS 滤波，所以得到的曲线往往滤去了很多噪音，比原始曲线更平滑。图 6 中(a)、(b)分别表示同一像元点的原始 LAI 时间序列(2001—2007 年)及用 DHR 预测的曲线与原始 LAI 及多年均值的比较。该像元点属于落叶林，该地类的 LAI 序列具有明显的季节变化，图 6(a)原始序列表明了该特点，同时由于获取数据、生长变化等问题，LAI 在生长的高峰期受噪音影响较大，该像元点的 2007 年 LAI 与多年平均 LAI 相关系数为 0.888；图 6(b)的预测曲线非常平滑，几乎滤掉了噪音造成的 LAI 值跳动，生长曲线形态预测较准，与多年均值生长曲线基本吻合，但由于原始 2007 年 LAI 曲线受噪音影响，因此预测精度并不高，R^2 只有 0.676。图 6(c)、(d)同样表示了同一像元点的原始及预测时间序列曲线，该像元点也具有明显季节性特点，因此预测的曲线形态比较符合原始情况。该像元点属于混交林地类，在生长期易受噪音影响，导致原始 LAI 曲线不平滑，图 6(c)显示该像元点有 2 个明显的生长高峰期且受噪音影响 LAI 值跳动很大，其 2007 年 LAI 与多年平均 LAI 相关系数为 0.919；图 6(d)图的 DHR 预测曲线将 2 个生长高峰很好地预测出来，且平滑噪音造成的 LAI 跳动，LAI 值大致与多年平均 LAI 近似，但由于形状与原始 2007 年 LAI 相差较大，因此预测精度 R^2 不高，只有 0.772。

从图 6 可以看出，原始序列受到噪音影响导致 LAI 曲线不平滑，有异常值存在，且 LAI 值跳动频繁的情况下，如果该像元点属于季节变化明显的地类，那么用 DHR 模型预测出来的曲线还是能很好地将生长曲线预测出来，而且还能平滑由于噪音造成的曲线跳动，得到的曲线更合理，更平滑。虽然由于形态与原始序列的数据相差较大造成预测精度 R^2 值不大，但从预测实际曲线来看，效果更好。

3.2.3　填充数据影响

在 MODIS 的 LAI 数据产品中经常由于各种原因造成数据缺失，为了避免缺失数据对分析造成很大影响，选用了一种滤波方法首先对数据进行补缺(Fang 等, 2008)。最后用来进行分析的序列是完整的，但是一些序列由于缺失数据过多，填充的数据很多是常数，因此原始序列的曲线并不很合理，这样的情况下用 DHR 模型进行预测，效果不好。在所分析的 9 个地类中，稀树草原、草地和灌木林地类的像元点有很多是填充数据较多的情况，而且由于噪音和这些地类本身 LAI 值变化范围较小等原因，所得到的预测结果并不理想。图 7 显示了两个例子，其中图 7(a)、(b)所示的像元属于草地地类，图 7(c)、(d)所示的像元属于灌木林地类。从图 7(a)、(c)的 LAI 原始序列看，属于这 2 个地类的像元点 LAI 值很低，在 1.0 以下，原始 LAI 序列的曲线有很多直线和跳动，因为这 2 个地类的数据除受噪音影响外，有很多缺失值，需要常数填充，造成得到的曲线并不符合自然形态，这 2 幅图中的 2007 年 LAI 与多年平均 LAI 的相关系数分别为 0.931 和 0.947，2007 年这 2

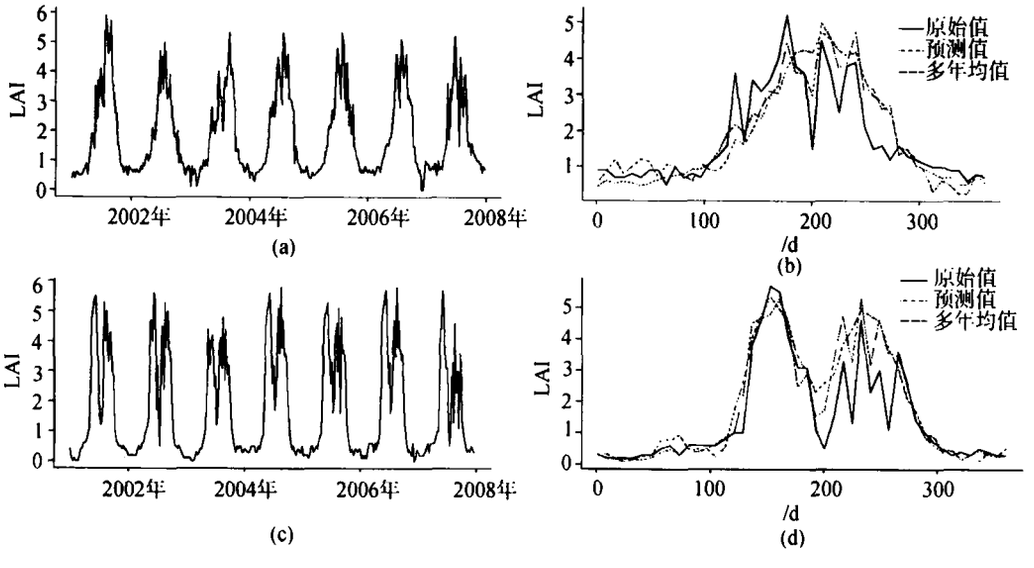

图 6　2 个不同地类像元点预测结果

(a) 落叶林类像元 LAI 原始时间序列 2001—2007 年; (b) 落叶林类像元 2007 年预测结果与原始数据比较; (c) 混交林类像元 LAI 原始时间序列 2001—2007 年; (d) 混交林类像元 2007 年预测结果与原始数据比较

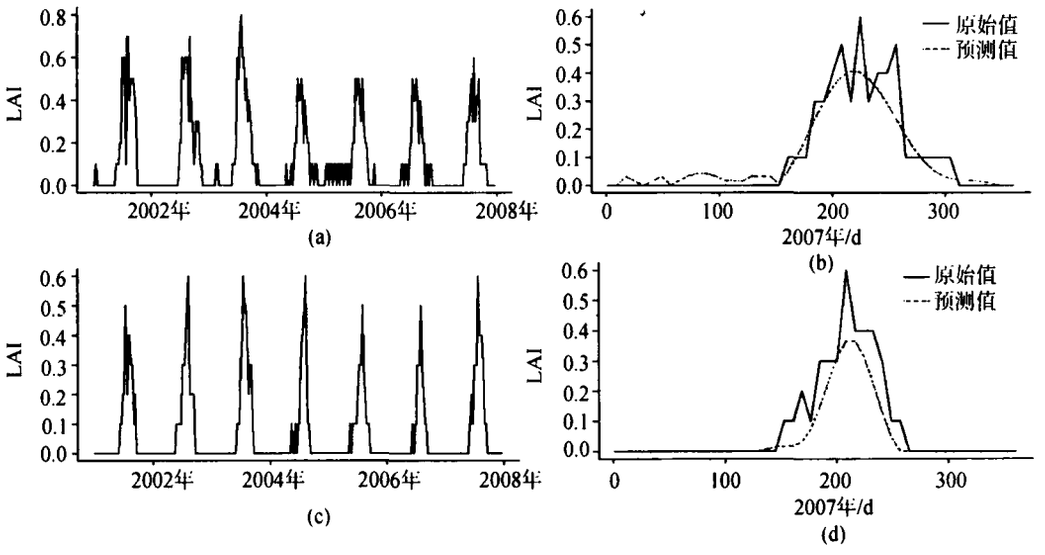

图 7 有填充数据的 LAI 时间序列预测结果

(a) 草地类像元原始 LAI 时间序列 2001—2007 年; (b) 草地类像元 2007 预测结果与原始数据比较; (c) 灌木林类像元原始 LAI 时间序列 2001—2007 年; (d) 灌木林像元 2007 预测结果与原始数据比较

个像元的生长曲线与前几年类似，说明这 2 个像元点 2007 年生长情况与往年相似；图 7(b)、(d)的预测曲线很好地平滑了噪音，而且比原始 LAI 曲线更吻合自然情况，但由于噪音等因素影响，预测值在生长高峰期均偏低，预测精度 R^2 为 0.861、0.824，说明形状差异较大会影响预测结果的计算精度。

从图 7 看出，在因缺失数据过多而用填充数据的情况下，如果原始序列季节变化比较明显，用 DHR 模型的预测结果使得噪声和填充值部分拟合平滑，更接近该像元类别 LAI 的时序变化特征。采用 DHR 模型有助于改进 MODIS LAI 数据产品的适用性。

3.3 DHR 模型拟合缺失数据

按照 DHR 模型的原理，它本身使用的 KF/FIS 滤波方法除了可以更好地进行预测，平滑噪音等，还可以直接处理有缺失的时间序列数据，拟合其中的缺失数据，但该模型只能用于有少量缺失数据的情况。为了更好地说明 DHR 模型的此功能，选择了 2 个像元点为例说明如下。

图 8 两个像元点分别属于落叶林及农作物地类。图 8(a)为落叶林地类像元点有缺失数据的时间序列，缺失点共 20 个，图 8(b)为用 DHR 模型拟合的数据及与原始数据的残差。从图 8(b)中清楚地看出，用 DHR 模型很好地拟合了缺失部分的数据，这部分缺失数据的拟合精度是 R^2=0.8344, RMSE=0.9306; 前面所有 6a 的数据在有缺失数据的情况下用 DHR 模型拟合的精度也很好，R^2=0.9376, RMSE=0.9305。图 8(c)为缺失了 2 段数据的 LAI 时间序列，该像元点属于农作物地类，缺失数据共 20 个，拟合结果在图 8(d)显示，有缺失数据的部分已经很好地与原始数据拟合，而且前 6a 的拟合数据比原始数据平滑，拟合数据与原始数据的残差较小，该点的缺失数据拟合精度 R^2=0.9565, RMSE=0.5338, DHR 拟合的所有 6a 数据与原始数据的拟合精度 R^2 达到 0.9401, RMSE=0.129。因此从该例子中可以证明在原始数据质量较好的情况下，DHR 对有少量缺失数据的序列有很好的拟合效果，且与原始序列缺失数据的位置无关，证明了 DHR 模型的适用性很广。

4 结 论

本文所研究的 DHR 模型，基于 UC 模型，每个成分用 State-Space 模型表示，其季节周期成分近似于傅里叶的谐波计算，但每个系数由能表达随时间变化理论的最常用的一种 SS 模型——GRW 模型来表示，通过所分析的时间序列的特点确定所用模型中的超参数及滤波所用“窗口”参数 NVR，最后由 KF/FIS 滤波得到时间序列的各成分，并可实现拟合和预测的功能。本文应用 DHR 模型，分析了 MODIS 的 LAI 长时间序列的产品，从分解、预测和缺失数据序列拟合等几个方面探讨了 DHR 模型对提取 LAI 遥感高级产品中周期变化和趋势变化成分的适用性。

本文首先讨论了 DHR 模型对时间序列中主要信息的提取，效果显示，提取出的趋势、季节等各成分可以表达时间变化特征，且能拟合出随时间变化

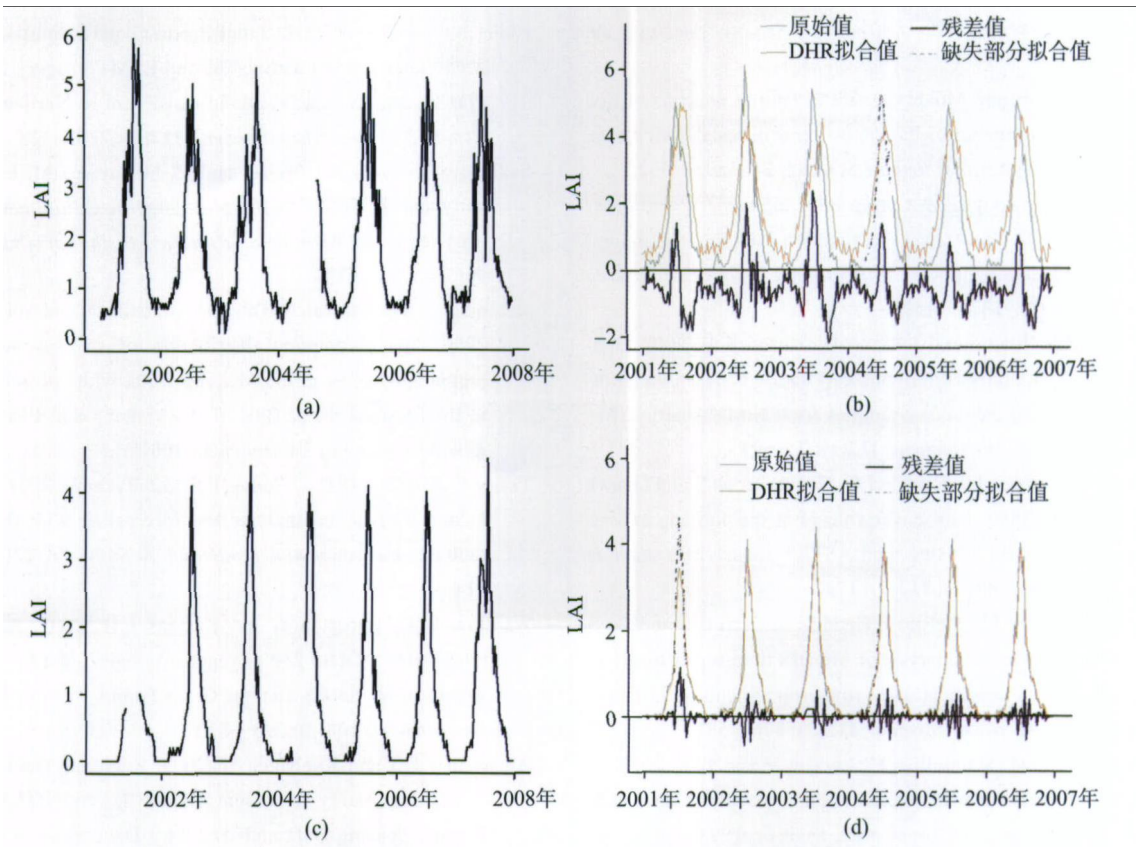

图 8　运用 DHR 模型拟合有缺失数据的 LAI 时间序列

(a)有 1 段缺失数据的落叶林类像元 LAI 时间序列 2001—2007 年; (b) DHR 模型拟合图 8(a)像元 LAI 时间序列 2001—2007 年; (c)有 2 段缺失数据的农作物类像元 LAI 时间序列 2001—2007 年; (d) DHR 模型拟合图 8(c)像元 LAI 时间序列 2001—2007 年

的模型(GRW 模型), 最后分离出的残差成分也基本接近白噪音分布。证明了 DHR 模型可以很有效地分解遥感 LAI 时间序列, 得到的各成分比较合理, 尤其是趋势部分。

通过对一共 896 个站点, 并属于 9 个地类的 MODIS 的 LAI 时间序列数据分别用 DHR 模型拟合并预测, 发现尽管对不同地类、或是不同情况下的像元, DHR 模型的预测结果会出现一些不一样的情况, 但在整体上对 LAI 产品是适用的, 且预测精度整体上较好。用 DHR 模型建模并进行预测时, 不需要事先知道原始序列的很多信息, 例如季节长度、一年生长季的个数等, 只需要通过该序列在频率域的谐波表现即可建立近似模型。该模型对原始数据质量较好、像元所属地类的季节变化比较明显的类别, 如农作物、落叶林、混交林等, 得到的预测精度很好。DHR 预测得到的 LAI 曲线比原始曲线更平滑, 形状也更自然合理。

本文还讨论了对于有少量缺失数据的时间序列, 用 DHR 模型进行补缺和拟合的情况。实验证明, DHR 对于有少量缺失数据且原始数据质量较好的时间序列拟合的精度很好, 不需要预先知道缺失数据的个数, 以及对应的具体位置, DHR 模型只根据已有序列在频率域的谐波表现建立模型, 最后由 KF/FIS 滤波得到完整的各成分的数据。图 8 两个例子中缺失数据的拟合精度达到了 0.8 以上, 且序列的所有数据用 DHR 模型的拟合精度达到了 0.9 以上。证明 DHR 模型可适用于有少量缺失数据的时间序列, 尤其是对于遥感产品这种很容易由各种原因造成数据缺失, 及易受噪音影响的情况, DHR 模型具有适用优势。

在研究中还存在一些问题, 如将所有像元的周期确定为 1a(即回归波谱阶数为 46), 某些地类的显著生长周期并不为 1a, 因此这个参数的设置会造成拟合模型不准确; 另外, 用确定谐波个数估计超参数和 NVR 的条件还需要更多检验, 以得到更好的经验判断值。

致　谢　感谢北京师范大学马斌同学提供预处理滤波数据。

REFERENCES

Alhamad M N, Stuth J and Vannucci M. 2007. Biophysical modelling and NDVI time series to project near-term forage supply: spectral analysis aided by wavelet denoising and ARIMA

modelling. *International Journal of Remote Sensing*, **28**: 2513—2548

Canisius F, Turral H and Molden D. 2007. Fourier analysis of historical NOAA time series data to estimate bimodal agriculture. *International Journal of Remote Sensing*, **24**: 5503—5522

Dash J, Mathur A, Foody G M, Curran P J, Chipman J W and Lillesand T M. 2007. Land cover classfication using multi-temporal MERIS vegetation indices. *International Journal of Remote Sensing*, **28**(6): 1137—1159

Fang H, Liang S, Townshend J R and Dickinson R E. 2008. Spatially and temporally continuous LAI data sets based on an integrated filtering method: Examples from North America. *Remote Sensing of Environment*, **112**(1): 75—93

French A N, Schmugge T J, Ritchie J C, Hsu A, Jacob F and Ogawa K. 2008. Detecting land cover change at the Jornada experimental range, New Mexico with ASTER emissivities. *Remote Sensing of Environment*, **112**(4): 1730—1748

Galford G L, Mustard J F, Melillo J, Gendrin A, Cerri C C and Cerri C E P. 2008. Wavelet analysis of MODIS time series to detect expansion and intensification of row-crop agriculture in Brazil. *Remote Sensing of Environment*, **112**(2): 576—587

Hüttich C, Herold M, Schmullius C, Egorov V and Bartalev S A. 2007. Indicator of Northern Eurasia's land-cover change trends from SPOT-Vegetation time-series analysis 1998—2005. *International Journal of Remote Sensing*, **28**(18): 4199—4206

Jakubauskas M E, Legates D R and Kastens J H. 2001. Harmonic analysis of time-series AVHRR NDVI data. *Photogrammetric engineering and remote sensing*, **67**(4): 461—470

Jakubauskas M E, Legates D R and Kastens J H. 2002. Crop identification using harmonic analysis of time-series AVHRR NDVI data. *Computers and Electronics in Agriculture*, **37**(1-3): 127—139

Lhermitte S, Verbesselt J, Jonckheere I, Nackaerts K, van Aardt J A N, Verstraeten, W W and Coppin P. 2008. Hierarchical image segmentation based on similarity of NDVI time series. *Remote Sensing of Environment*, **112**(2): 506—521

Liu L L and Xu H M. 2007. The NDVI change rules of the main vegetations in HuangHe basin and the relationships with the meterologic factors. *Chinese Agriculture Meterology*, **28**(3): 334—337

Mao F, Hou Y Y, Tang S H, Zhang J H and Lu Z G. 2007. Meadow classifying and dynamic changing studying in the Northern Tibetan based on the remote sensing data of 20 years. *Ecological applications*, **18**(8): 1745—1750

Ng C N and Young P C. 1990. Recursive estimation and forecasting of non-stationary time series. *Journal of Forecasting*, **9**(2): 173—204

Pedregal D J and Trapero J R. 2007. Electricity prices forecasting by automatic dynamic harmonic regression models. *Energy Conversion and Management*, **48**(5): 1710—1719

Pedregal D J and Young P C. 2006. Modulated cycles, an approach to modelling periodic components from rapidly sampled data. *International Journal of Forecasting*, **22**(1): 181—194

Röder A, Hill J, Duguy B, Alloza J A and Vallejo R. 2008a. Using long time series of Landsat data to monitor fire events and post-fire dynamics and identify driving factors. A case study in the Ayora region (eastern Spain). *Remote Sensing of Environment*, **112**(1): 259—273

Röder A, Udelhoven T, Hill J, del Barrio G and Tsiourlis G. 2008b. Trend analysis of Landsat-TM and-ETM+ imagery to monitor grazing impact in a rangeland ecosystem in Northern Greece. *Remote Sensing of Environment*, **112**(6): 2863—2875

Sakamoto T, Yokozawa M, Toritani H, Shibayama M, Ishitsuka N and Ohno H. 2005. A crop phenology detection method using time-series MODIS data. *Remote Sensing of Environment*, **96**(3-4): 366—374

Sakamoto T, Van Nguyen N, Ohno H, Ishitsuka N and Yokozawa M. 2006. Spatio–temporal distribution of rice phenology and cropping systems in the Mekong Delta with special reference to the seasonal water flow of the Mekong and Bassac rivers. *Remote Sensing of Environment*, **100**(1): 1—16

Taylor C J, Pedregal D J, Young P C and Tych W. 2007. Environmental time series analysis and forecasting with the Captain toolbox. *Environmental Modelling & Software*, **22**(6): 797—814

Wardlow B D, Egbert S L and Kastens J H. 2007. Analysis of time-series MODIS 250 m vegetation index data for crop classification in the US Central Great Plains. *Remote Sensing of Environment*, **108**(3): 290—310

Weissteiner C J and Kuhbauch W. 2005. Regional Yield Forecasts of Malting Barley (Hordeum vulgare L.) by NOAA-AVHRR Remote Sensing Data and Ancillary Data. *Journal of Agronomy and Crop Science*, **191**(4): 308—320

Westra T. 2007. Monitoring Sahelian floodplains using Fourier analysis of MODIS time-series data and artificial neural networks. *International Journal of Remote Sensing*, **28**(7): 1595—1610

Young P C, Pedregal D J and Tych W. 1999. Dynamic harmonic regression. *Journal of Forecasting*, **18**(6): 369—394

Young P C, Taylor C J, Tych W and Pedregal D J. 2007. The Captain Toolbox. Centre for Research on Environmental Systems and Statistics, Lancaster University, UK., Internet: www.es.lancs.ac.uk/cres/captain

Young P. 1989. Recursive estimation, forecasting and adaptive control. Control and Dynamic Systems, **30**, 119—166

Zhang M W, Qingbo Z, Zhongxin C, Jia L, Yong Z and Chong Fa C. 2008. Crop discrimination in Northern China with double cropping systems using Fourier analysis of time-series MODIS data. *International Journal of Applied Earth Observations and Geoinformation*, **10**(4): 476—485

Zhang X, Rui S, Bing Z and Tong Q X. 2008. Land cover classification of the North China Plain using MODIS_EVI time series. ISPRS Journal of Photogrammetry and Remote Sensing, **63**(4): 476—484

Zhao Y S. 2003. Principles and Methods of Analyzing in Remote Sensing Applications. Beijing: Science Publisher

附中文参考文献

刘绿柳, 许红梅. 2007. 黄河流域主要植被类型 NDVI 变化规律及其与气象因子的关系. 中国农业气象, **28**(3): 334—337

毛飞, 侯英雨, 唐世浩, 张佳华, 卢志光. 2007. 基于近 20 年遥感数据的藏北草地分类及其动态变化. 应用生态学报, **18**(8): 1745—1750

赵英时. 2003. 遥感应用分析原理与方法. 北京: 科学出版社